

UNCLASSIFIED

AD 263 500

*Reproduced
by the*

**ARMED SERVICES TECHNICAL INFORMATION AGENCY
ARLINGTON HALL STATION
ARLINGTON 12, VIRGINIA**



UNCLASSIFIED

DISCLAIMER NOTICE

THIS DOCUMENT IS THE BEST
QUALITY AVAILABLE.

COPY FURNISHED CONTAINED
A SIGNIFICANT NUMBER OF
PAGES WHICH DO NOT
REPRODUCE LEGIBLY.

NOTICE: When government or other drawings, specifications or other data are used for any purpose other than in connection with a definitely related government procurement operation, the U. S. Government thereby incurs no responsibility, nor any obligation whatsoever; and the fact that the Government may have formulated, furnished, or in any way supplied the said drawings, specifications, or other data is not to be regarded by implication or otherwise as in any manner licensing the holder or any other person or corporation, or conveying any rights or permission to manufacture, use or sell any patented invention that may in any way be related thereto.

363500

A large, bold, black and white logo consisting of two stylized letters 'B' stacked vertically. The logo is rendered with a high-contrast, graphic style, using thick black lines and white space. It is positioned in the center of the page.

MEMORANDUM REPORT NO. 1349
AUGUST 1961

A COMB FILTER FOR USE IN TRACKING SATELLITES

ARPA Satellite Fence Series

61-4-5

XEROX

Richard L. Vitek

ASTIA

ASTIA
PAPUAPNG
OCT 27 1961
TIPUR

Report Number 24 in the Series

Department of the Army Project No. 503-06-011
Ordnance Management Structure Code No. 5210.11.143
BALLISTIC RESEARCH LABORATORIES



ABERDEEN PROVING GROUND, MARYLAND

BALLISTIC RESEARCH LABORATORIES

MEMORANDUM REPORT NO. 1349

AUGUST 1961

A COMB FILTER FOR USE IN TRACKING SATELLITES

ARPA Satellite Fence Series

Richard L. Vitek

Ballistic Measurements Laboratory

Report Number 24 in the Series

Department of the Army Project No. 503-06-011
Ordnance Management Structure Code No. 5210.11.143

ABERDEEN PROVING GROUND, MARYLAND

BALLISTIC RESEARCH LABORATORIES

MEMORANDUM REPORT NO. 1349

RLVitek/bst
Aberdeen Proving Ground, Maryland
August 1961

A COMB FILTER FOR USE IN TRACKING SATELLITES

ABSTRACT

This report presents the design and evaluation of a 180 element comb filter. This unit was developed in conjunction with the ARPA Satellite Fence program for the detection and tracking of non-radiating satellites. The primary purpose of this comb filter is to detect and measure the frequency of short duration Doppler signals in the presence of noise. The filter elements have a bandwidth of 10 cps and are spaced 20 cps apart to cover a 3800 cps frequency range. A multiple pen analog recorder is used to record individual filter outputs. The evaluation includes data on simulated as well as actual satellite signals.

TABLE OF CONTENTS

	Page
INTRODUCTION	7
SYSTEM AND COMB PARAMETERS	9
FILTER CONSIDERATIONS	11
FILTER DESIGN	14
CIRCUIT DESIGN	16
TESTS AND EVALUATION	31
APPENDIX I, BIBLIOGRAPHY OF REPORTS IN THE BRL-DOPLOC SERIES	35

INTRODUCTION

The Ballistic Research Laboratories have been engaged in tracking satellites since the first Sputnik on October 4, 1957. This tracking was accomplished with the DOPLOC (DOploc Phase LOCk) system. Tracking, in this case, means the reception of radio frequency signals and the recording of their frequency versus time characteristics. The frequency shift is a result of the Doppler effect associated with a moving source. The received signals were so weak that a phase-locked tracking filter was required to separate the signal from the noise. The signals were obtained either directly from a satellite borne transmitter (active) or indirectly from a ground transmitter by reflection from the satellite (passive). A very brief description of DOPLOC will be presented here as a background for the comb filter requirements. The block diagrams presented have been greatly simplified and equipment not directly related to the comb filter has been omitted.

Figure 1a is a block diagram of the DOPLOC receiving system for tracking active satellites. With the signals received from active satellites, low gain broadbeam antennas were used with a manually locked narrow bandwidth tracking filter. The filter had bandwidths from 0.5 to 50 cps which gave a signal-to-noise (S/N) improvement up to 42 db. This unit provided a clean, continuous output Doppler signal. The results obtained with this system were excellent. Continuous Doppler signals were received throughout the passage of satellites from horizon to horizon. Multiple satellites were tracked by having a tracking filter for each signal. Figure 1b shows a typical Doppler data curve of frequency versus time.

With the advent of passive tracking, the DOPLOC system was extended to include illuminating the satellite and receiving reflected Doppler signals. Because of the relatively weak received signals in the passive or reflection system, high gain, narrow fan beam antennas had to be employed. The Interim DOPLOC Satellite Fence stations, as set up in September 1959 under ARPA sponsorship, contained three, fixed, $8^{\circ} \times 80^{\circ}$ beamwidth antennas with the same type of receivers and phase-locked

filters used with the active satellite tracking system. This system, shown in Figure 2A, no longer produced continuous data but gave three portions of the Doppler curve as shown in Figure 2B. Received signals above the noise threshold lasted 5 to 8 seconds in the center beam and 15 to 20 seconds in the north and south beams. These signal durations were so short that manual lock-on of the tracking filter was no longer feasible. An automatic system was designed which located the desired signal and locked the tracking filter to it. This automatic lock-on system functioned reasonably well, but it did not provide maximum sensitivity or acquisition capability.

The final system as proposed to ARPA is shown in Figure 3A. This system contained a $1.4^{\circ} \times 40^{\circ}$ scanning fan beam antenna. The scan rate was high compared to the satellite rate of travel and data were to be obtained at short intervals throughout the curve as shown in Figure 3B. The phase-locked tracking filter was no longer compatible with this type (short duration) signal, even with the use of an automatic lock-on system. A new filter-recorder combination was required which could locate and record short duration signals. This lead to the development of the comb filter herein described.

SYSTEM AND COMB PARAMETERS

System Considerations

The comb filter design is related to the electrical noise and signal environment in which it must operate. This environment can be divided into three parts; desired signal, noise, and spurious signals. These signals are determined by the DOPLOC system parameters. Therefore, a more detailed look at the DOPLOC system is required to determine its output signal characteristics.

A major advantage of the DOPLOC Satellite Fence is its inherent ability to provide all of the orbital parameters from the data obtained during a single pass of a satellite. A minimum of twelve data points are considered necessary to provide an adequate orbital solution. Therefore, the antenna configuration and motion, which determine the number of data points, must be tailored to provide at least twelve data points. In addition to this restriction, there are three other basic parameters which determine the signal conditions. They are the carrier frequency, the satellite velocity, and the slant range to the satellite. A carrier frequency of 108 mc and satellite velocity of 300 miles per minute give a Doppler frequency shift of approximately 12 kc. All three parameters determine the rate of change of frequency, which, at closest approach, is 25 cps/s at a satellite altitude of 1000 miles and 100 cps/s at 100 miles altitude. The maximum rate of change of frequency of 100 cps/s determines the minimum usable bandwidth of 10 cps. This bandwidth in turn sets the time available to recognize a signal at 100 milliseconds. This time of 100 milliseconds determines the maximum scan rate for a given antenna beamwidth. Since twelve data points are required on each pass, there is also a minimum scan rate associated with the low altitude passes. If the antenna scan is made fast enough to obtain at least twelve points, where each point is 100 milliseconds in duration, an antenna beamwidth of 1.4 degrees is required. To summarize, the desired signal characteristics are, a 12 kc frequency shift, a maximum rate of change of frequency of 100 cps/s, and a signal duration of 100 milliseconds.

Spurious Signals

In addition to the desired signal, there are other signals which are present and important. In a reflection system using a high power ground transmitter, forward tropospheric scatter generally occurs to some extent. Field experience indicates that this feedthrough level can be equal to the receiver noise level. This signal, although fixed in frequency, must be considered in the filter design.

Meteors also present a problem. Here, field experience indicates that two types of echos are present, a head echo and a trail echo. The head echo will cover the entire Doppler frequency range at a very high rate of change of frequency. The trail echo is relatively fixed in frequency and of large amplitude. The trail echos generally occur near the center of the Doppler frequency band. The head echos are discriminated against to a large extent because of their high rate of change of frequency.

Noise Bandwidth and Amplitude

Noise bandwidth and noise level considerations are of prime importance. The noise bandwidth is important in that the overall bandwidth reduction determines the dynamic range required of the comb filter. The noise level must be considered both from the standpoint of absolute level and variation of level. With a given, fixed, bandwidth reduction, the noise level determines the minimum usable signal level. The variation in level is important in the automatic gain control (AGC) design. The R 390/A receiver used in the DOPLOC system has a maximum I. F. bandwidth of 16 kc, which is adequate to cover the 12 kc Doppler frequency shift. The maximum audio signal, without any danger of clipping, is one volt r.m.s. The noise level is a function of the receiving antenna orientation with respect to cosmic noise sources, as well as the receiver gain. An overall variation of 5 to 1 in noise voltage output of the receiver is possible due to the combined variations of cosmic noise and receiver gain.

FILTER CONSIDERATIONS

Ideal and Practical Filter for Sine Waves

Once the input signal characteristics have been defined, the performance characteristics desired for the comb filter may be outlined. The basic comb filter is a multiplicity of narrow band elements distributed uniformly through a given frequency band. This is shown graphically in Figure 4A. The problem may be better understood by first examining an ideal filter and comparing its operation with the actual filter. Consider an individual ideal element as shown in Figure 4B to be 10 cps wide with a flat top and having infinite side slope attenuation. This 10 cps filter is placed in a recording circuit as shown in Figure 4C. The circuit contains the filter, an amplifier of gain K, and threshold circuit and a recorder. The recorder is an go no-go device. The threshold and recorder combination are such that the input to the threshold circuit must equal or exceed a given level E_{TH} for the recorder to operate. Let us make one further stipulation that the circuit have unlimited dynamic range. These conditions describe an ideal circuit element. To further simplify the problem, let us consider the effectiveness of the circuit to separate only two sine wave signals; first, E_D , the desired signal, whose frequency is contained within the bandwidth and second, E_{UD} , the undesired signal, with variable amplitude and frequency but outside the bandwidth. What, if any, restrictions does this ideal circuit present to these two signals?

With an ideal filter with infinite side slopes at the input, the undesired signal may be as close to the band edges as possible and as large in amplitude as desired and it will never present any interfering output signal within the desired bandwidth. Thus, there is no minimum amplitude restriction on E_D as a function of E_{UD} . Also, as long as we are willing to make the gain K large enough to amplify E_D to E_{TH} , E_D has no minimum level. E_D also has no maximum level. The signals may be as small or as large as desired and still be recognized, and each will operate only one circuit element.

Let us replace the ideal filter with one of finite side slope of x db/octave, and center frequency f_o , as shown in Figure 5A, and consider its effect on the frequency and amplitude characteristics of E_D and E_{UD} . We select some arbitrary minimum level for E_D , say y db, and plot E_{UD} as a function of frequency which will provide a signal level of y db at f_o . This is shown in Figure 5B. Since we have an attenuation of x db/octave, a signal of $y + x$ db one octave above or below f_o will be attenuated to y db. Similarly, for two octave separation, E_{UD} can be $y + 2x$ db and so forth. Therefore, if the signal at f_o due to E_{UD} must always be smaller than y , there is a limit to the value of E_{UD} as a function of its frequency proximity to f_o . In addition to the interference produced within a given bandwidth, a large signal can activate a number of circuit elements in proportion to its amplitude. This is shown in Figure 5C. A signal amplitude of $y + nx$ db will be attenuated x db/octave and will cover n octaves before going below the minimum level of y db. This will operate all the circuit elements contained in n octaves, which is undesirable when reading the data. If only one circuit element is to operate per signal, some type of AGC system is required. To summarize, a non-ideal filter requires AGC and places a restriction on the ratio of E_{UD}/E_D as a function of frequency.

Effect of Noise

Let us consider the final condition of separating signal from noise. We assume first that the noise is uniformly distributed throughout the frequency band. Then, no matter which type of filter is used or where it is positioned in the frequency band, it will contain noise. Therefore, there is always some noise introduced into the system. The amount of noise is a function of the total noise power and the ratio of the input bandwidth to the filter bandwidth. In this case, the input bandwidth and the filter bandwidth are fixed so that the noise output of the filter is directly proportional to input noise. The minimum level of E_D is a function of the noise out of the filter. Let us assume for the moment that E_D minimum is equal to the noise level out of the filter. This then makes E_D minimum directly related to total input noise. With noise in the system we can no longer define E_D arbitrarily or even as a given voltage level. It must be defined in terms of a S/N ratio with respect to the input or output

noise. To be consistent, then, we should define E_D maximum and E_{UD} maximum in terms of the noise level as a reference. Thus, we can see that the introduction of noise into a circuit using a non-ideal filter places restrictions on all the input signals.

Recording Data

A number of methods are available for recording the output of the comb filter. In the works here described, a multiple pen, paper chart recorder was used. There is one pen for each filter element. Since there is no scanning involved, no time is lost searching for the signal. This gives the additional capability of recording multiple satellites simultaneously.

FILTER DESIGN

Overall Comb Filter

Having defined the input signal characteristics and the relation between these signals and a general form of narrow band filter, the overall comb may now be outlined in block form. Starting with the minimum block, any necessary items may be added as needed. Figure 6A shows the basic receiver with the three variables, E_D , E_{UD} , and E_N as output signals, and a recording element. We denote the signals out of the receiver by the subscript R and the signals out of the filter by the subscript F, and consider these three variables and their effect on the design of the comb. First, we consider the noise voltage E_N . Since there is always some noise out of the filter, the gain K is limited to a value which brings E_{NF} just below the threshold level. Now we assume a given ratio of E_{DR}/E_{NR} which gives a ratio E_{DF}/E_{NF} of one. E_{DF} then is the minimum signal that will just operate the recorder. We consider now the effect of the receiver gain decreasing by a factor of two. The input S/N ratio, E_{DR}/E_{NR} , remains fixed, but E_{DF} has decreased by a factor of two. If K is fixed, then E_{DF} will no longer operate the recorder. It now requires a larger S/N ratio than before. If the receiver gain increases, the noise will operate the recorder. Thus, to obtain maximum sensitivity, that is minimum S/N ratio, and no extra readouts due to noise - the noise level must remain fixed just below the threshold level. Therefore, a constant noise input must be provided to the filter with some type of AGC system. The conventional AGC maintains a constant r.m.s. output by adjusting the sum of the noise plus signal to be a constant. A large undesired signal will cause the receiver gain to be decreased and produce the undesirable effect of reducing the noise output. An AGC based on noise only, which will maintain a constant noise output even in the presence of a large signal, is necessary. Figure 6B shows this noise AGC circuit added to the comb. Having determined previously that the noise out of the receiver can vary as much as 5 to 1 and that the maximum level is one volt r.m.s., the noise AGC circuit must be designed to handle from 0.2 to 1.0 volts r.m.s. input and produce a constant output.

Let us consider the effect of the other variables E_D and E_{UD} in the non-ideal filter. Large values of the sine waves will not be controlled by the noise AGC, but they must be controlled if they are to operate only one filter. At this point we consider the signal AGC as acting on all the filters. If the signal AGC circuit operates on the basis of input amplitude, then pre-filter AGC is not possible. This is so because the input signal can be very small compared to the noise and still be capable of operating more than one filter. This small signal cannot be recognized in the noise on the basis of amplitude. The post filter signal is always larger than the post filter noise and it is at this point that we must develop the AGC voltage. If the signal AGC is developed from all the filters on the basis of total signal and applied to a common amplifier, then only the largest signal will be read. This is not desirable. AGC must be developed on each board and applied to only those boards which would have given an ambiguous output, and preferably in an amount which is proportional to the received signal in each board. Fig. 6C shows the complete comb with individual signal AGC on each element. The methods of applying this AGC will be covered later.

Number of Elements

The next step is to determine the number of elements needed in the comb. This is a question of how many filters are needed in the 12 kc frequency band. Considering that there are a minimum number of data points available, and each lasts the minimum time, each point must be read. Complete coverage of the 12 kc band would require filters at 10 cps spacing. Since each filter element is fairly complex, a complete system would represent a considerable investment. It was decided to try a token number of filters to prove the system before expanding to the total 1200. This trial comb was selected to cover only 3600 cps at 20 cps spacing with 180 filters. Its input can be switched three times to cover the entire 12 kc band.

Having determined the overall block diagram for the system the individual blocks can be developed in detail.

CIRCUIT DESIGN

Receiver Noise AGC

A need for an AGC circuit which is activated by noise only has been discussed. Actually, it is impossible to make a circuit which is sensitive to noise only. The best approach appears to be one which gives the maximum rejection to the interfering sine waves. This rejection can be on the basis of amplitude, time, or frequency. Amplitude rejection is not feasible because the interference can be larger than the noise, thus we must depend on a time or frequency discrimination.

Let us consider first time discrimination. Up to this point consideration has been given to the total change in noise level but not the rate of change of level. The change in noise level is basically due to effective sky temperature change with antenna orientation. An antenna scan from horizon to horizon requires fifteen seconds. Thus, a time constant of one second for the AGC will permit the gain control voltage to follow the noise. However, the desired signals of 0.1 second duration will have little effect on the AGC because they are not present long enough. Meteor trail echos and signals received via scatter propagation from the transmitter which are present for long periods will not be rejected by an AGC system with a 1 second time constant.

We now consider what frequency discrimination will do. Feedthrough (signals arriving via tropospheric propagation), is always present at a fixed frequency. If the noise is sampled in a narrow frequency band it is possible to exclude the feedthrough altogether. The probability of receiving trail echos is also reduced considerably.

Thus, it can be seen that time discrimination will eliminate short duration signal interference, and frequency discrimination will eliminate most of the feedthrough and meteor interference. Figure 7 shows a block diagram of the circuit. The noise plus signal go through the gain controlled amplifier to two outputs, the output to the filter bank and the output to the control circuit. The amplifier is followed by a filter at a center frequency of 6 kc with a bandwidth of 160 cps. The total noise bandwidth is 16 kc, so a reduction of noise in the filter of 10 to 1 occurs. However, a signal in

this bandwidth is not reduced at all. Therefore, a S/N ratio of 1 at the input to the 160 cps filter would result in a S/N ratio of 10 at the output of the filter, which would give too much weight to the signal. It is necessary to follow the 160 cps filter with an amplifier-limiter combination. The noise level is adjusted to approximately one-half of full output and any signal is then limited to twice the value of the noise. This procedure still gives more than adequate range for variation in noise level to operate the AGC amplifier. The limiter is followed by a rectifier, to convert the signal to a d.c. voltage, and a d.c. amplifier to provide loop gain. There is sufficient gain in the loop to handle a 20 to 1 variation of the input with less than a 10 percent change in the output of the controlled amplifier. The integrator provides the time constant which is one second. The value of the time constant is chosen to minimize the effect of signals with a duration shorter than one second. For example, a 0.1 second duration signal large enough to produce a d.c. output of twice the noise level would try to charge to twice the noise voltage level. However, it is present for only 0.1 second and would not increase the voltage more than 10 percent. Without AGC, the decrease in sensitivity would have been at least 40 percent for a S/N of 1 and greater for larger S/N ratios. The only type of signal which could cause interference would be a long duration trail echo. By reducing the bandwidth we have reduced the probability of this occurring. All other signal effects from feedthrough, short duration desired signals, and high rate head echos are reduced considerably.

Q MULTIPLIER

Basic Feedback Circuit

The 10 cps narrow band filter is in the form of a Q multiplier using standard L and C components. Since the frequency band to be covered is 2 kc to 14 kc, Q's range from 200 to 1400 to provide the 10 cps bandwidth at the various frequencies. With nominal coil Q's in the order of 100, multiplication is from 2 to 14. The problem was to design a small compact circuit capable of providing these Q's with as much stability as possible. An analysis was made of Q multiplier circuits to determine the best design criteria. Basically, any LC oscillator circuit with the positive feedback below the oscillating point will, if used as an amplifier, produce an increase in the Q. However, the question is, how stable is this new Q value, assuming nominal stability of the variables involved. Before this can be resolved, the circuit action which produces the multiplication must be understood.

Two types of feedback circuits were compared, one in which the feedback factor, B, is positive only and the other, where B is a composite of positive and negative feedback. In both cases the positive B network uses an LC resonant circuit.

Let us consider first the basic feedback circuit, as shown in Figure 8, in which B is fixed. E_i is the input voltage to the whole circuit, E_1 is the input to the amplifier of gain K, and B is the feedback factor. Equations 1, 2, and 3 can be written by inspection.

$$E_1 = E_1 + E_{fb} \quad (1)$$

$$E_1 K = E_2 \quad (2)$$

$$E_2 B = E_{fb} \quad (3)$$

Substituting (2) and (3) into equation (1) gives

$$E_2 / K = E_1 + E_2 B \quad (4)$$

Rearranging equation (4) gives the form

$$E_2 \left(\frac{1}{K} - B \right) = E_1$$

$$E_2/E_1 = K/(1-BK) = K' \quad (5)$$

This is the form of the standard feedback equation where K' is the closed loop gain. Normally in this type of circuit, B is fixed with frequency and K' is investigated with respect to changes in K . However, in the Q multiplier it is B which is variable. Figure 9 shows the basic Q multiplier in which B is positive and the B network is a resonant circuit. If we consider the B network with E_2 as constant in amplitude but variable in frequency, then E_{fb} will vary as the LC circuit goes through resonance. Since B is defined as being the ratio of E_{fb} to E_2 , B will also vary with frequency. The variation of B with frequency is shown in Figure 10. The 3 db bandwidth is determined by the loaded Q of the resonant circuit.

Q Multiplier as a Function of the Output Voltage

If the Q multiplier can be evaluated in terms of the output voltage then it can later be defined in terms of B and K . In Figure 9, if the feedback circuit is disconnected at point x and a curve is drawn of output versus frequency, curve A in Figure 11 would be obtained. Then, upon re-connecting the circuit, draw a second curve of output versus frequency and curve B would be obtained. Since the feedback is positive, curve B would be larger in amplitude. It is noted that curve B has been adjusted in amplitude so that the intersection of the two curves is at E_0 which is the 3 db point on curve A. Also, the 3 db bandwidth, Δf_2 , of curve B is smaller than the 3 db bandwidth, Δf_1 , of a curve A. If we denote the Q of curve B, Q_2 , and the Q of curve A, Q_1 , then the Q multiplier, M , is the ratio of the Q's as shown in equation (6).

$$M = Q_2/Q_1 = \Delta f_1/\Delta f_2 \quad (6)$$

Let us denote the peak value of curve A, E_{R1} , and the peak of curve B, E_{R2} . If the assumption can be made that R_1 and R_2 in Figure 9 are greater than the Z of the resonant circuit, then the voltages are directly proportional

to the Q's and:

$$\frac{E_{R2}}{E_{R1}} = Q_2/Q_1 \quad (7)$$

By substituting $E_{R1} = 1.4 E_o$ into equation (7):

$$\frac{E_{R2}}{E_o} 1.4 = Q_2/Q_1 = M \quad (8)$$

This defines the multiplier in terms of the change of output voltage from E_o to E_{R2} .

Q Multiplier in terms of B and K

Curve A in Figure 11 and the Beta curve of Figure 10 are both drawn for the same circuit Q; therefore E_o represents the output E_2 with 0.7B and E_{R2} the output with full B. Equations 9 and 10 give the closed loop gain with 0.7B and B, respectively.

$$K'_2 = K/(1 - .7BK) \quad (9)$$

$$K'_1 = K/(1 - BK) \quad (10)$$

Equations 11 and 12 give E_{R2} and E_o in terms of the closed loop gains.

$$E_1 K'_2 = E_o \quad (11)$$

$$E_1 K'_1 = E_{R2} \quad (12)$$

Substituting equations 11 and 12 into equation 8 gives:

$$K'_1/1.4 K'_2 = M \quad (13)$$

$$\text{Let } K'_1/K'_2 = A \quad (14)$$

$$\text{Then } A/1.4 = M \quad (15)$$

"A" is then the variable part of the multiplier M and will determine the stability of the new Q. "A" can now be expressed in terms of B and K by substituting equations 9 and 10 into equation 14.

$$A = \frac{K}{1-BK} / \frac{K}{1-.7BK} = 1 + \frac{.3BK}{1-BK} \quad (16)$$

Figure 12 shows a plot of A versus BK. As BK approaches 1, A approaches infinity and the circuit will oscillate. It will be noted that the useful

values of A lie in the range of BK from 0.95 to 0.999. This means that the circuit is always relatively close to the oscillating point. Even with a low value of A of 6, a 5 percent change in B or K would cause oscillations. B, which is made up of passive elements, can easily be held to one percent or less. However, K which is the open loop gain is not nearly as stable, and in transistor circuits would be especially difficult to maintain. A circuit configuration which is relatively independent of K would be much more desirable, and this is the second circuit to be discussed.

The second circuit contains two loops, one positive and one negative, and is shown in block form in Figure 13. In this configuration the negative feedback is fixed and the positive feedback varies as before. The total feedback, B, is the algebraic sum of the negative and positive B's. The equations at resonance and at the 3 db point are as follows:

$$\text{at resonance the total } B_t = B_+ + B_- \quad (17)$$

$$K'_1 = K/(1 - B_t K) \quad (18)$$

$$\text{at the 3 db point } B'_t = 0.7B_+ + B_- \quad (19)$$

$$K'_2 = K/(1 - B'_t K) \quad (20)$$

By rearranging equation 17 and 19 and substituting into equation 20, K'_2 may be expressed in the following form:

$$K'_2 = K/(1 - B_t + 0.3 B_+) \quad (21)$$

A, which is the ratio of K'_1/K'_2 , may be expressed in terms of BK as:

$$A = 1 - B_t K + \frac{0.3 B_+ K}{1 - B_t K} = 1 + \frac{0.3 B_+ K}{1 - B_t K} \quad (22)$$

At this point a restriction must be made that B_t may never be positive. Then rearranging equation 22, by multiplying the second term by B_t/B_t ,

$$A = 1 + \frac{0.3 B_+ B_t K}{B_t - 1 - B_t K} \quad (23)$$

It will be noted that as K approaches infinity, the term $B_t K/(1 - B_t K)$ approaches unity as a limit. A then approaches the value $1 + 0.3 B_+ / B_t$. Figure 14 shows a plot of equation 23 as A versus $K B_t$ for various values of B_+ / B_t . One can see that A in this case is relatively independent of $K B_t$ as long as $K B_t$ is

kept above 25. A is, however, very dependent on the ratio B_+/B_t . If the B networks, which are made up of passive elements, are held to close tolerances, the circuit will be very stable. It is virtually independent of K as long as K is large.

Description of Final Circuit

Figure 15 shows the schematic of this second circuit, which is the circuit as used in the filter bank. The negative loop is made up of R_8 and R_6 . The positive loop is R_{10} and R_2 in series, plus the resonant circuit. The basic amplifier is d.c. coupled and R_8 and R_6 provide negative d.c. as well as negative a.c. feedback. This helps to stabilize the d.c. operating point considerably. The circuit is very tolerant of any variations in transistors. The Zener diode was added instead of a dropping resistor to provide additional gain. R_4 and C_3 form a necessary phase correction network to stop oscillation caused by the large amount of negative feedback. Frequency is adjusted with the choice of coil and capacitors, and the Q is adjusted by setting the positive feedback level with R_2 .

Measurement of Q is difficult at the higher frequencies when one attempts to measure ± 5 cps at 12,000 cps. A method was devised to use an oscilloscope and speed up this measurement. If the response of a resonant circuit to a step function is calculated, the envelope has the form,

$$\text{Amplitude of Envelope} = S = E e^{-at} \quad (24)$$

where $a = R/2L$, R is the series resistance of the coil and L is the inductance of the coil. Since $Q = 2\pi fL/R$, at resonance,

$$a = R/2L = \pi f/Q = \pi \Delta f, \quad (25)$$

where Δf is the bandwidth between 3 db points.

This equation is the same as the standard equation expressing the charge of a capacitor. The time constant in this case would be equal to $1/a$. The time constant can then be expressed as:

$$T = \text{time constant} = 1/\pi \Delta f \quad (26)$$

If a signal at the center frequency of the resonant circuit is applied whose amplitude is in the form of a step function and a measurement is made of the time response, we have a measure of the bandwidth. The time constant is 32 milliseconds for all of the filters, irrespective of the frequency of the

of the filter. This method has the advantage of permitting measurement of bandwidths less than 1 cps with ease and speed compared to the 3 db method. Tests indicated that 1/2 cps bandwidths could be obtained before approaching the oscillating point. This (1/2 cps bandwidth) gives a multiplication of approximately 200 as the ultimate capability. Since the largest multiplication needed was 14, all of the filters were operating well away from the oscillating point.

SIGNAL AGC

Signal Control and AGC Distribution

The need has been previously determined for a post-filter signal AGC circuit. We have also seen that the filter used in this case will be a resonant circuit. This section will deal with the gain controlled amplifier, the generation of the control voltage and the distribution of this voltage among the filters of the filter bank.

Assume an ideal delayed AGC which starts to operate with a signal just above the threshold level and has an output d.c. voltage which is directly proportional to the input a.c. voltage. Now consider the distribution of this d.c. voltage to the other filters. To do this visualize a group of filters with an input signal in the center filter. For ease of description, let us call the center filter A and the other filters as they progress away on either side of A, B, C, D, and so forth. This is shown in Figure 16A. There will be some signal voltage at all the filter inputs due to the signal at the input of filter A. Since all the filters are resonant circuits, and of the same bandwidth, distribution of the voltage at each of the inputs is in the form of a resonance curve as shown in Figure 16B. The dashed line with an amplitude of X represents the threshold level. All the filters contained within the resonance curve above the threshold level would be actuating the recorder.

Since the d.c. output voltage is directly proportional to a.c. input voltage, Figure 16B also represents the AGC d.c. output of each filter. Filter A, which contains the signal at its frequency, has the largest d.c. output. This voltage can be distributed to the other filters with a resistive network, always to be larger than the AGC developed in the other filters. This is shown by the dotted lines in Figure 16B. The circuit can also be arranged to have the larger of the two AGC voltages control the gain in each filter. This will then cut off all of the filters except filter A. The resistive network is made in the form of a symmetrical ladder attenuator with equal sections. Since all of the filters are connected together with identical sections, the distribution of voltage is not peculiar to a

particular set of filters. The voltage will be distributed as shown on both sides of the strong signal, no matter which filter the signal frequency matches. This type of circuit has the advantage of keeping a minimum number of filters cut off. As an example, Figure 17 shows two main signals X and Y of different amplitudes and their AGC curves. The frequency covered is a small portion of the total 4 kc band. Each signal cuts off a number of filters in proportion to its amplitude. Yet, a signal such as A contained within the cut off region but larger than the distributed d.c. voltage will still be read. Any signal not in the cut off region can be read with maximum sensitivity. Thus, it is possible for meteors, feedthrough, and many desired signals to be present simultaneously and still read each one by the operation of a single pen per signal.

Circuit Analysis

In the general description of the AGC action, several points were mentioned and assumed to be true without giving any proof. These were; the linearity of a.c. input to d.c. output, the cut off action of the distributed voltage, and the design of the ladder attenuator. These items will now be taken up in turn.

Linearity of a.c. Input Versus d.c. Output

Figure 18 shows a combined block and schematic form of the AGC circuit. The d.c. control voltage E_{DC} is fed back across the series connected resistor R_1 and diode D_1 . This voltage determines the current and thus the resistance of D_1 . C_1 is a very low impedance to the operating frequency and acts only as a d.c. blocking device. D_1 , in series with R_2 to the input voltage E_{IN} , determines the voltage E_2 available to the fixed gain amplifiers which follow.

The forward drop across a diode is relatively independent of the current through it and for practical purposes can be considered a constant. If I represents the current through the diode, and R_D the resistance of the diode, then this constant voltage drop may be expressed as:

$$I R_D = \text{constant} = A \quad (27)$$

It can also be expressed in the form:

$$\frac{E_{DC}}{(R_1 + R_D)} = I \quad (28)$$

If R_1 is much larger than R_D then equation 28 reduces to:

$$\frac{E_{DC}}{R_1} = A \quad (29)$$

Substituting equation 29 in equation 27 we have:

$$\frac{E_{DC}}{R_D} \frac{R_D}{R_1} = A \quad (30)$$

Since R_1 is fixed in value equation 3 can be written in terms of a new constant as:

$$\frac{E_{DC}}{R_D} R_D = A R_1 = B = \text{constant} \quad (31)$$

If it is further assumed that there is sufficient loop gain to maintain the output of the a.c. amplifier constant, then:

$$\begin{aligned} E_o &= \text{constant} = E_2 G_2 \\ E_2 G_2 &= E_{IN} \frac{R_D}{R_D + R_2} G_2 \end{aligned} \quad (32)$$

If R_2 is larger than R_D then:

$$E_o = E_{IN} \frac{R_D}{R_2} G_2 = C \quad (33)$$

Since G_2 , R_2 , and E_o are all fixed in value,

$$E_o R_2 / G_2 = \text{constant} = E_{IN} R_D = D \quad (34)$$

Substituting the value of R_D from equation 31 into equation 34 gives:

$$\begin{aligned} E_{IN} \frac{B/E_{DC}}{R_2} &= D \\ E_{IN} &= D/B E_{DC} = K E_{DC} \end{aligned} \quad (35)$$

Equation 35 shows E_{DC} to be a linear function of E_{IN} .

Cutoff Action of AGC

It is readily apparent that we can feed back a voltage which is larger than the AGC voltage on any given filter, but it would appear that this voltage would merely reduce the gain and not cut off the filter. The following discussion will show how the cutoff action takes place. Figure 19 gives a plot of two curves, curve A, the a.c. input versus the d.c. control voltage, and curve B, the a.c. input versus the threshold gain. By threshold gain is meant that gain which is required to give an output at the threshold level from the AGC controlled amplifier. Let S represent the signal in filter A, and P represent the signal in filter B. At signal level P, Q represents the AGC voltage developed and R is the gain required to bring P up to the threshold level. However, T represents the AGC voltage at filter A and U shows that portion which is fed back from filter A to filter B. If the voltage U controls filter B then it will produce gain V which is lower than gain R, and filter B will no longer have adequate gain with input P to reach the threshold level. This feedback voltage will work in a similar manner for all the other filters.

Ladder Attenuator

Figure 20 shows the network and filter connections. Let us consider only a part of the network as shown in Figure 20b. Let E_1 be the input voltage and E_2 , E_3 , and E_4 be the voltages down the attenuator. Since each section has an impedance Z , then:

$$\frac{E_2}{E_1} = Z/(R_1 + Z) = \frac{E_3}{E_2} = \frac{E_4}{E_3} = X \quad (36)$$

There is a fixed loss ratio of X as one progresses down the network. Equation 36 can be rearranged to give R_1 as a function of Z and X .

$$R_1 = Z (1 - X)/X \quad (37)$$

Using only one section of the network as shown in Figure 20c, Z can also be written equal to the parallel combination of R_2 and R_1 plus Z in series:

$$Z = \frac{(R_2)(R_1 + Z)}{R_2 + (R_1 + Z)} \quad (38)$$

Substituting equation 37 in equation 38 gives:

$$\begin{aligned} Z &= R_2 \frac{Z}{X} / (R_2 + \frac{Z}{X}) \\ R_2 &= Z / (1 - X) \end{aligned} \tag{39}$$

Thus, equations 37 and 39 give R_1 and R_2 in terms of Z and X , where Z is determined by circuit impedances and X is a function of the distribution desired. Figure 21 shows the resonance curve (a) as well as the distribution curves for several values of X . The final choice of X is somewhat arbitrary, however, there are some circuit considerations. To be sure that the larger voltage always controls the AGC, a diode D_2 was added as shown in Figure 18. To obtain the best circuit operation, one must always maintain a few tenths of a volt back bias across D_2 . This requires that X must be chosen so that the curve is high enough at its extremities. X is not a fixed value, since the resistor R_2 is actually the parallel combination of R_3 and the filter resistance, as shown in Figure 20A. This input resistance is variable with signal level and will vary from 20K with large signals to 1 Megohms with small signals. This condition is helpful since it produces larger values of X with small signals which will occur at the extremities of the curve.

In this particular case, linearity of the signal in the AGC amplifier is not too important. However, it is important in the noise AGC amplifier. The input voltage across the diode must be kept below 50 millivolts to keep distortion at a minimum.

Threshold Circuit

This section covers the threshold circuit and the relation of the S/N ratio to the threshold level. Up to this point the minimum usable signal was considered as one which produced a S/N ratio of unity past the 10 cps filter. Actually this is the theoretical limit which we would like to achieve, but never quite realize in practice. This is best explained by reference to the block diagram and the various signal levels which occur as shown in Figure 22. The signal and noise are rectified, filtered, and then go to a differential amplifier. The other input to the differential amplifier is a reference level which determines the threshold level. When the rectified input exceeds the threshold level the recorder writes.

The signals are presented pictorially below the block diagram of Figure 22. At the input to the rectifier shown in (A) we have the signal whose frequency is f_c , and the noise which contains the frequency components between $f_c - 5$ cps and $f_c + 5$ cps. The next set (B), shows the full wave output of the rectifier. Up to this point the signal is in the frequency range between 2 kc and 6 kc. Set (C) shows the output of the low pass filter. It is seen that the signal d.c. component is clean because all of the ripple components are high compared to 10 cps and are removed. The noise, however, consists of all frequencies between $f_c - 5$ cps and $f_c + 5$ cps and its rectified output contains all the difference frequencies between the noise components in this band, that is, 0 to 10 cps signals. The rectified noise output then contains a d.c. component and ripple in the 0 to 10 cps region. The next set, (D), shows two conditions, one, when both signal and noise are present and just equal to the threshold level, and the other when the same amount of noise is present but without signal. In the first case the noise ripple causes the voltage level to go below the threshold which causes a miss in the output when the signal is present. The second case shows the noise ripple exceeding the threshold and giving a false data pulse when the signal is not present. The total number of false alarms which can be tolerated depends on the read out system. The general approach to eliminate these errors is to lower the noise and increase the signal, as shown in

Figure 22 E, to minimize the occurrence of misses and false alarms. This, of course, calls for a better S/N ratio and lowers the overall sensitivity of the system. The actual loss can only be determined by experience with field data on a particular system. Since the final system has not been constructed, a firm figure is not available. However, general tests indicate that a loss of 6 db to 9 db could be expected.

TESTS AND EVALUATION

General

A brief description of the tests performed on the comb filter is given in this section. Initial tests for stability of the frequency and Q of the filter disclosed a need for temperature control. The relay rack used to house the filters and power supplies was equipped with blowers, heaters and a thermostat to provide temperature control. A temperature range of from 92 to 98 degrees F was maintained with this system. This was adequate to maintain the frequency of the filters within ± 2 cps and the Q within 10 percent of design values. However, the threshold level and threshold gain had a 3 to 6 db variation in sensitivity between individual filters. As the following figures, 33 through 34, show not all of the filters begin to write at the same signal level. This sensitivity effect is most noticeable when viewing the noise background, which shows light and dark lines instead of uniform gray lines. This effect can be eliminated by a modification of the d.c. amplifiers in the filters and recorder, but was not done on the prototype because of the time required to make the change.

Since the main use of the comb was for tracking satellites, tests were made for specific satellite tracking problems, as well as general problems. The following figures show simulated satellite signals as well as actual satellite signals obtained from field station magnetic tape records. In Figures 23 through 34 the paper was moving vertically at 0.1 inch per second, so the vertical axis represents time. The pens are spaced horizontally across the paper and each pen is connected to a filter, the filters being spaced 20 cps apart. Each presentation is then a frequency versus time graph. A total of 120 filters were used in the tests, giving a total range from 2 kc to 4.4 kc.

Simulated Signals

As mentioned in the previous section, the relation of the noise level to the threshold level is determined by the type of recording system to be used with the filter. The first test was to determine the optimum noise

level for maximum signal-to-noise ratio, as is shown in Figure 23. Signal was mixed with noise and applied to the input of the filter. The noise level was maintained fixed while the frequency of the input sine wave was varied from 2 kc to 4.4 kc. During the sweep, the amplitude of the sine wave was varied in amplitude in three steps, which divide the sweep into three equal parts. The sine wave amplitude steps used were - 27 db, -30 db, and -33 db with respect to the noise in all cases. The noise levels were from 100 millivolts to 250 millivolts as shown in the figure. By inspection of Figure 23 it is easy to see that the 150 millivolt noise level is optimum. These tests were made using a 20 kc bandwidth noise source and the 10 cps filters. With this combination, and input signal-to-noise of -33 db would provide a post filter signal-to-noise ratio of one. It is seen that at the 150 millivolt noise level some points are still readable at the -33 db sine wave level. With noise levels above 150 millivolts the system becomes saturated with the noise, and at lower levels the system becomes less sensitive. However, in the scanning beam antenna tracking system, which provides fewer data points, it would not be possible to read the data at the optimum sensitivity noise level. There would be hundreds of noise points for each data point. In the interest of trying to anticipate the loss of sensitivity associated with fewer data points, Figure 24 shows higher post filter signal-to-noise ratios. Figure 24 is similar to Figure 23 except that the noise levels vary from 100 mv to 70 mv and the signal levels vary from -21 db to -30 db. In the scanning beam system, data points would have been obtained every 15 seconds or 1.5 inches apart on the graph paper. If one used the criterion that there should be approximately the same number of data points as there are noise points then the 70 mv noise level with a -21 db sine wave level would be about the right choice. This is 9 db less sensitive than the optimum case which was anticipated.

One very important feature is the response of the filter to a signal with a high rate of change of frequency. Tests were run on the comb filter to indicate the minimum usable signal for a given rate of change of frequency in cps/s. The results are shown in Figure 25. It is interesting

to note that a loss of sensitivity did not occur until a rate exceeding Δf^2 was reached, and that rates in excess of 100,000 cps/s could be seen with a signal-to-noise ratio of one at the input to the filter.

The next test, shown in Figure 26, was with various signal levels to test the action of the signal AGC. Signals from -30 db to + 6 db with respect to the noise were used. The AGC performed well up to 0 db. At + 6 db the system began to overload as indicated by the dark traces in the background noise. Figures 27 and 28 show the action of the AGC with two signals present. Figure 27 shows a strong fixed frequency signal at -6 db level. By noting the background noise it can be seen that this signal is strong enough to cut off the noise from 18 filters and the chart appears clear on both sides of the strong signal. The second signal is a sweeping frequency with amplitude levels from -12 db to -30 db. It can be seen that the stronger signal at -12 db overrides the cutoff action of the -6 db fixed signal, but the weaker does not. Figure 28 shows two signals crossing simulating the data from two satellites tracked simultaneously. Since they are at the same amplitude all of the points are readable on both curves.

Satellite Signals

During the time that the satellite fence was in operation, many active and passive satellite signals were recorded on magnetic tape. These magnetic tapes were used to produce the chart records shown in Figures 29 through 34. As a means of comparison with the methods used at the APRA stations, chart records are shown of the same satellite passes that were tracked with the ALO-tracking filter combination. Section "A" of each figure is the record made with the comb filter, and section "B" is the ALO-tracking filter record. Figures 29 through 33 show satellite 1960 Delta revolutions 124, 140, 156, 165, and 172. Figure 34 shows an active track of Jupiter C during the launch phase. The arrows on the figures indicate the frequency limits of the tracking filter records. In general, the comb filter tracked the signal for a longer period. This was expected since the best sensitivity of the ALO

was -21 db, and could not pick up the signal as soon. However, after a lock was obtained the tracking filter was independent of the ALO and its sensitivity was identical to the comb filter.

The signals on the tapes had a frequency range from 2 kc to 12 kc. It was necessary to mix the tape signals with a signal from an oscillator to provide the comb filter with frequencies in the 2 kc to 4 kc range. Tests with simulated signals on the mixer indicated a 6 db loss in the S/N ratio as a result of the mixing. Therefore, in comparing the two types of records, the signal level for the comb filter should always be taken as 6 db less than that for the ALO record.

Summary

The test records of simulated and actual satellite signals show that the comb filter prototype has met all of the design requirements. If this unit had been expanded to the full compliment of 1200 filters it would have provided an effective tracking capability for the scanning antenna system. This model has proven the advantages and disadvantages of this type of system. It provides an excellent answer to tracking short duration, high rate of change of frequency signals.

Richard L. Vitek
RICHARD L. VITEK

BRL-DOPLOC REPORTS

No. 1 BRL Memo Report No. 1055 - October 1958, Doppler Signals and Antenna Orientation for a Doppler System, by L. P. Bolgiano, Jr. **CONFIDENTIAL**

No. 2 BRL Memo Report No. 1185 - January 1959, First Semi-Annual Technical Summary Report, Period 1 July 1958 - 31 December 1958, by L. G. deBey, V. W. Richard, A. H. Hodge, R. B. Patton, C. L. Adams. **CONFIDENTIAL**

No. 3 BRL Tech Note No. 1265 - June 1959, Orbital Data Handling and Presentation, by R. E. A. Putnam. **UNCLASSIFIED**

No. 4 BRL Tech Note No. 1266 - July 1959, An Approach to the Doppler Satellite Detection Problem, by L. G. deBey. **CONFIDENTIAL**

No. 5 BRL Memo Report No. 1220 - July 1959, Second Semi-Annual Technical Summary Report, Period 1 January - 30 June 1959, by L. G. deBey, V. W. Richard and R. B. Patton. **CONFIDENTIAL**

No. 6 BRL Tech Note No. 1278 - September 1959, Synchronization of Tracking Antennas, by R. E. A. Putnam. **UNCLASSIFIED**

No. 7 BRL Memo Report No. 1237 - September 1959, A Method of Solution for the Determination of Satellite Orbital Parameters from DOPLOC Measurements, by R. B. Patton, Jr. **UNCLASSIFIED**

No. 8 BRL Memo Report No. 1093 - March 1960, The Dynamic Characteristics of Phase-Lock Receivers, by Dr. Keats Pullen. **UNCLASSIFIED**

No. 9 Station Geometry Studies for the DOPLOC System, Stanford Research Institute. **UNCLASSIFIED**

No. 10 Final Report, Part B, Stanford Research Institute - July 1960, DOPLOC System Studies, by W. E. Scharfman, H. Rothman, H. Guthart, T. Morita. **UNCLASSIFIED**

No. 11 Philco Corporation - 4 May 1960, Polystation Doppler System. **UNCLASSIFIED**

No. 12 Space Science Laboratory, General Electric Co. - October 1960, Orbit Determination of a Non-Transmitting Satellite Using Doppler Tracking Data, by Dr. Paul B. Richards. **UNCLASSIFIED**

No. 13 Final Technical Report - University of Delaware - June 15, 1960, Quantum Mechanical Analysis of Radio Frequency Radiation, by L. P. Bolgiano, Jr. and W. M. Gottschalk. **UNCLASSIFIED**

No. 14 Final Report F/157, Columbia University - February 11, 1960, Summary of the Preliminary Study of the Applicability of the Ordin System Techniques to the Tracking of Passive Satellites. UNCLASSIFIED

No. 15 BRL Report No. 1110 - June 1960, Precision Frequency Measurement of Noisy Doppler Signal, by W. A. Dean. UNCLASSIFIED

No. 16 Third Technical Summary Report - Period July 1959 thru June 30, 1960, BRL Memo Report No. 1207, by A. L. deBey. UNCLASSIFIED

No. 17 Columbia University Tech Report No. T-1/157 - August 1, 1959, The Theory of Phase Synchronization of Oscillators with Application to the DOPLOC Tracking Filter, by E. Kreindler. UNCLASSIFIED

No. 18 BRL Tech Note No. 1345 - August 1960, DOPLOC Receiver for Use with Circulating Memory Filter, by K. Patterson. UNCLASSIFIED

No. 19 BRL Tech Note No. 1345 - October 1960, Parametric Pre-Amplifier Results, by K. Patterson. UNCLASSIFIED

No. 20 BRL Tech Note No. 1367 - December 1960, Data Generation and Handling for Scanning DOPLOC System, by Ralph E. A. Putnam. UNCLASSIFIED

No. 21 BRL Report No. 1123 - February 1961, The DOPLOC Instrumentation for Satellite Tracking, by C. L. Adams. UNCLASSIFIED

No. 22 BRL Memo Report No. 1330 - March 1961, DOPLOC Observations of Reflection Cross Sections of Satellites, by H. T. Lootens. UNCLASSIFIED

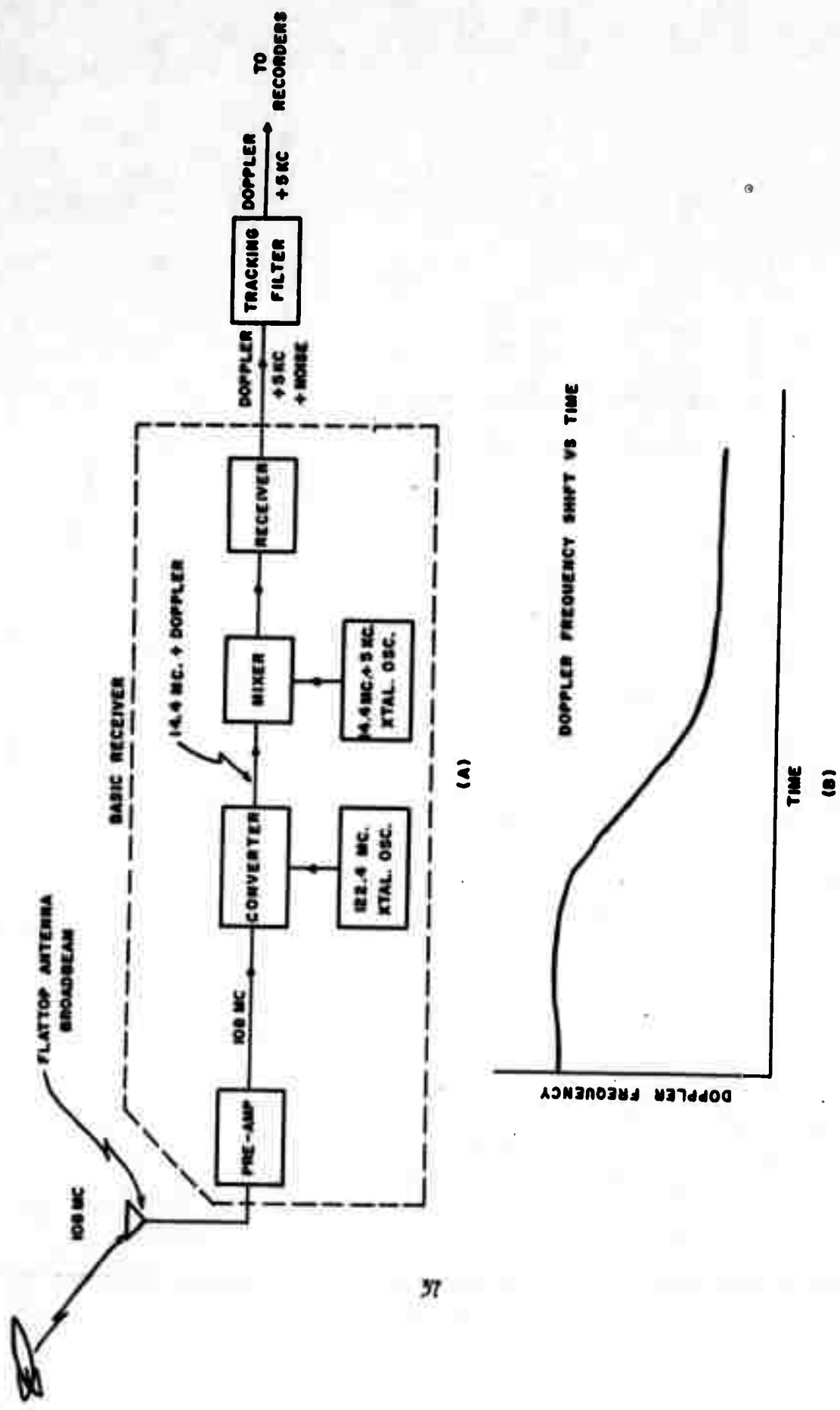
No. 23 BRL Memo Report No. 1362 - August 1961, Satellite Induced Ionization Observed with the DOPLOC System, by H. T. Lootens. UNCLASSIFIED

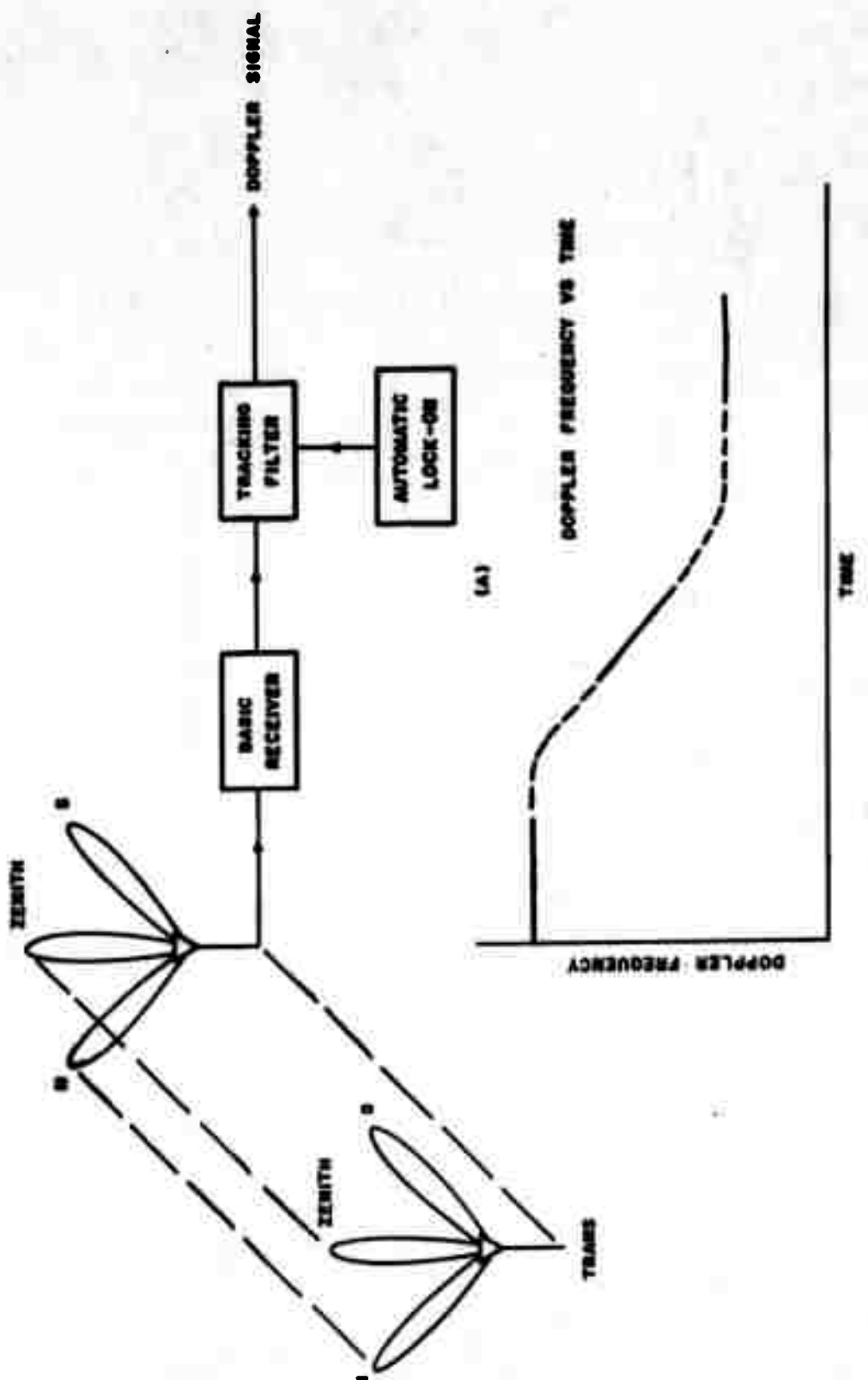
No. 24 BRL Memo Report No. 1349 - August 1961, A Comb Filter for Use in Tracking Satellites, by Richard Vitek. UNCLASSIFIED

No. 25 Final Summary Report on the BRL-DOPLOC Project - July 1961, by A. H. Hodge and R. B. Patton, Jr. UNCLASSIFIED

FIG. 1

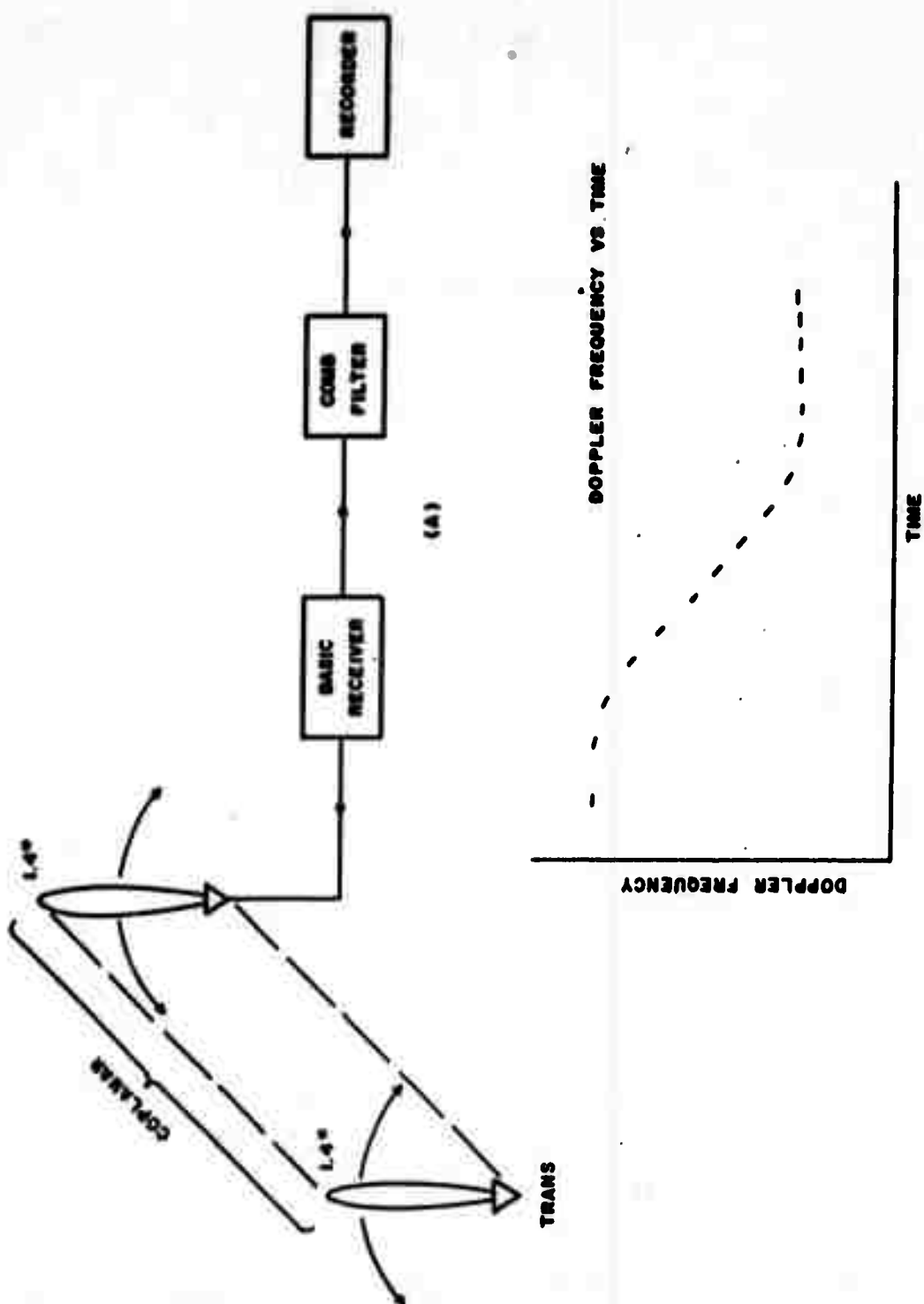
DOPLOC 108 MC RECEIVING SYSTEM





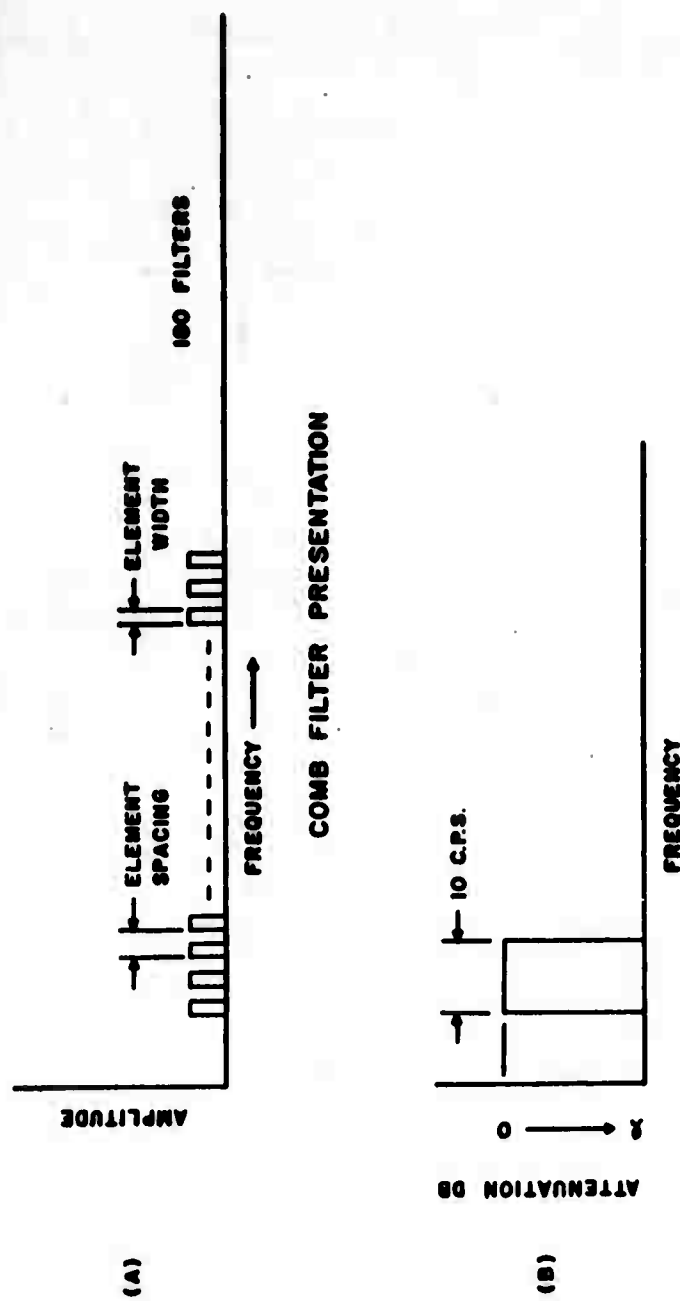
INTERIM DOPLOC FENCE RECEIVING SYSTEM

FIG. 2

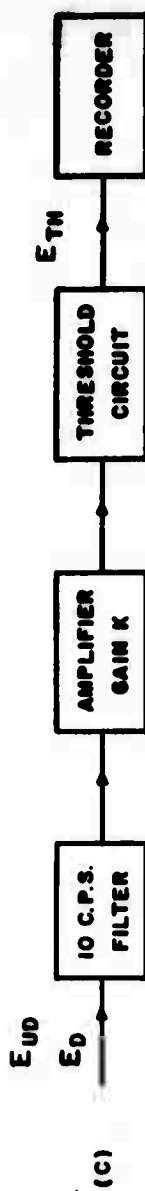


SCANNING ANTENNA BEAM RECEIVING SYSTEM

FIG. 3



FREQUENCY VS ATTENUATION OF
IDEAL 10 C.P.S. FILTER



FILTER AND RECORDER BLOCK DIAGRAM

FIG. 4

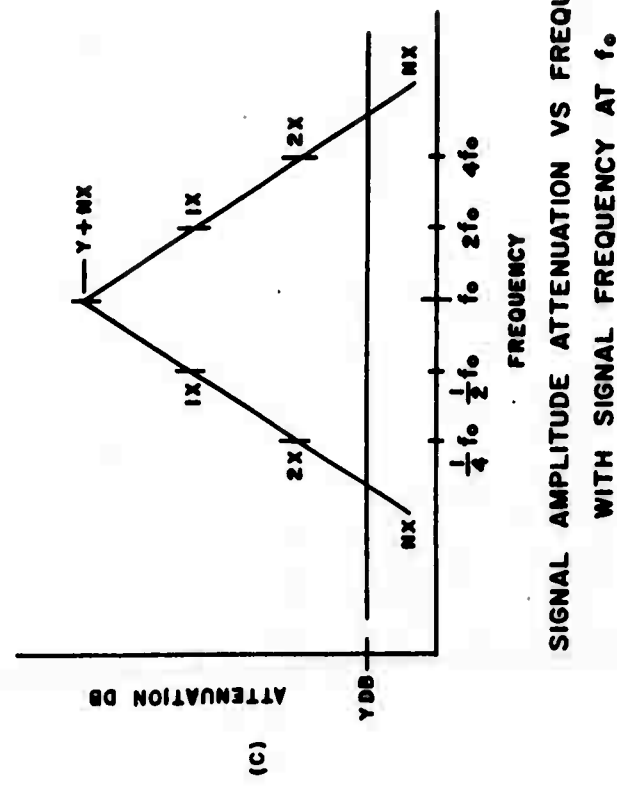
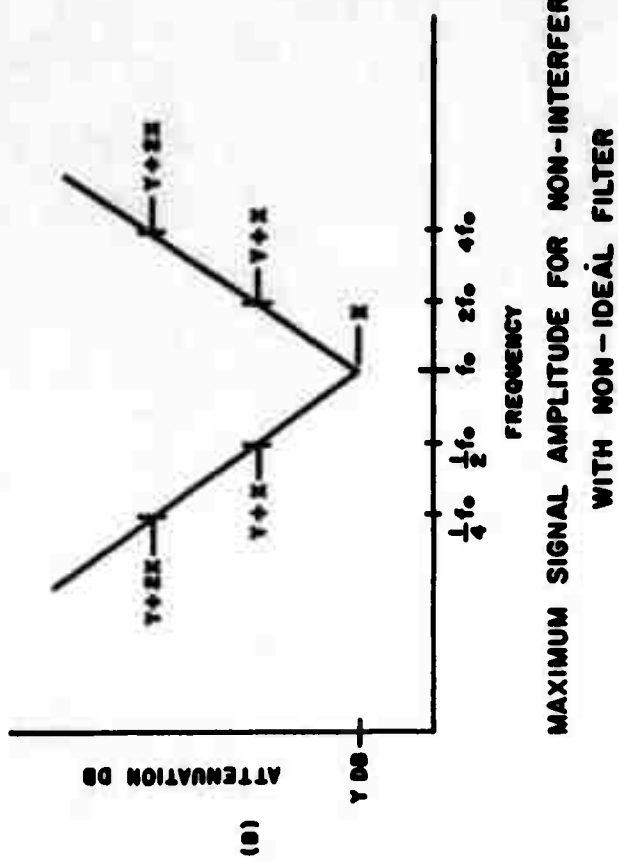
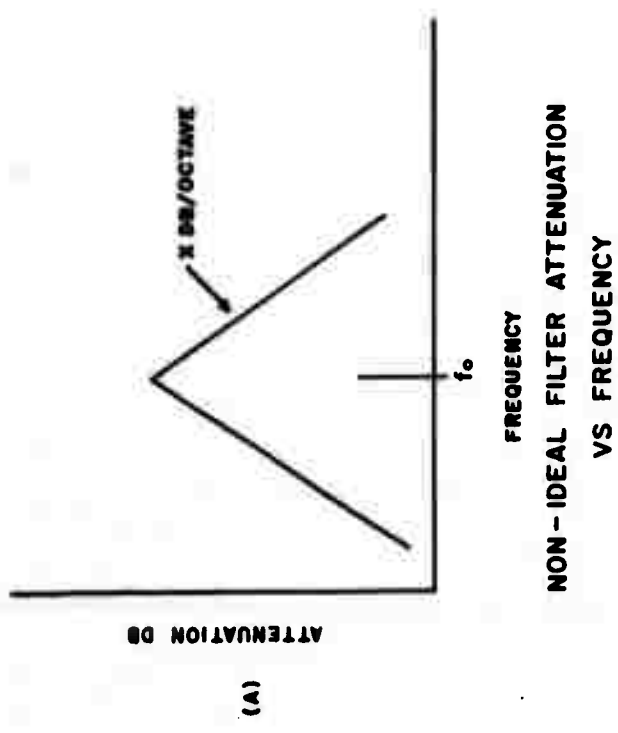
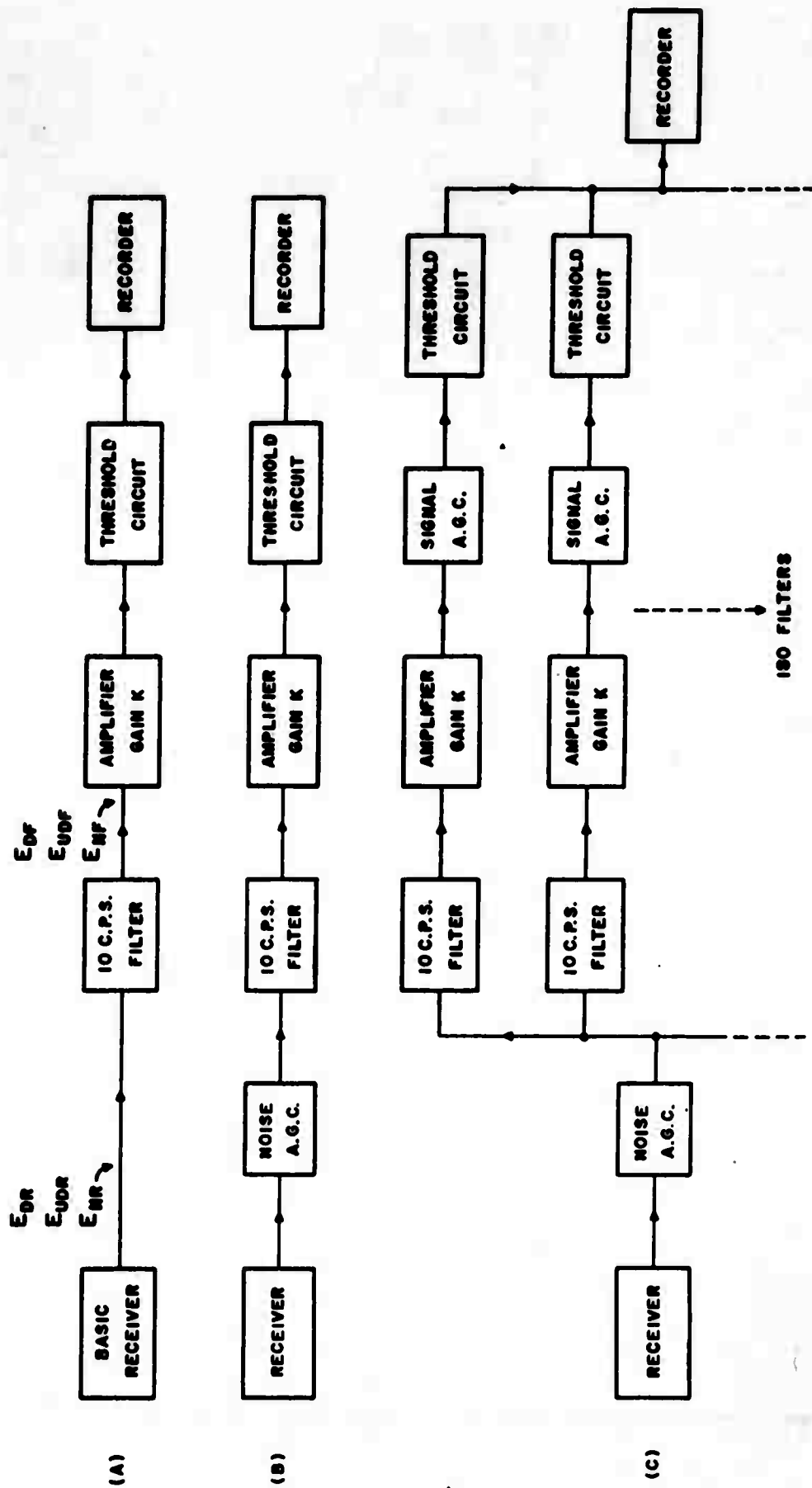
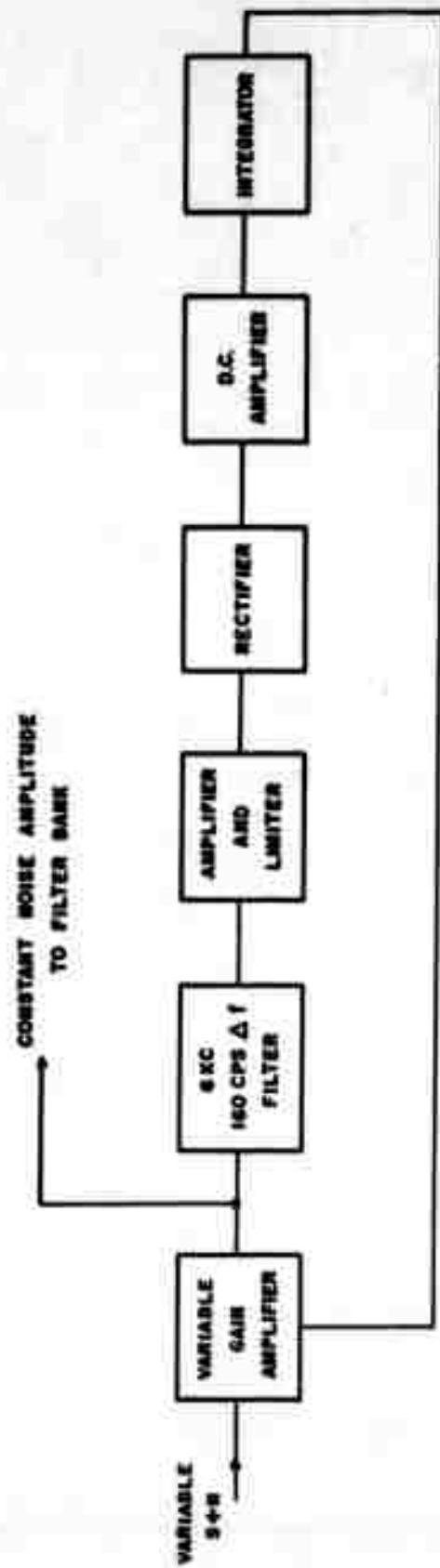


FIG. 5

OVERALL COMB FILTER BLOCK DIAGRAM

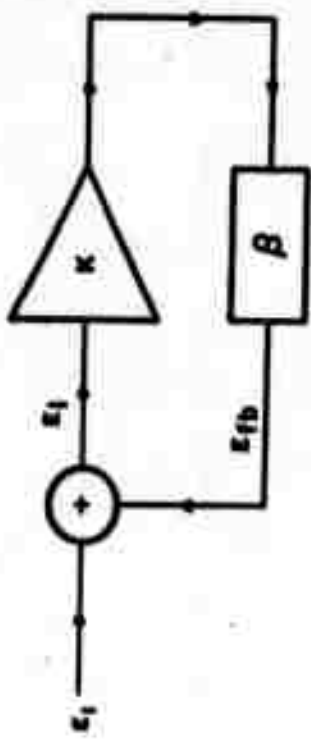
FIG. 6





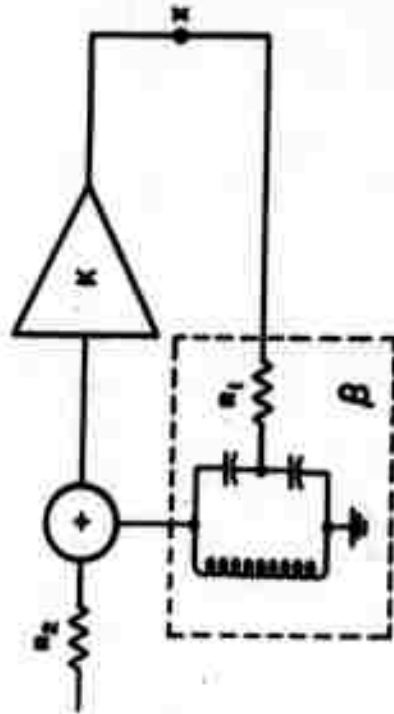
NOISE A.G.C. CIRCUIT BLOCK DIAGRAM

FIG. 7



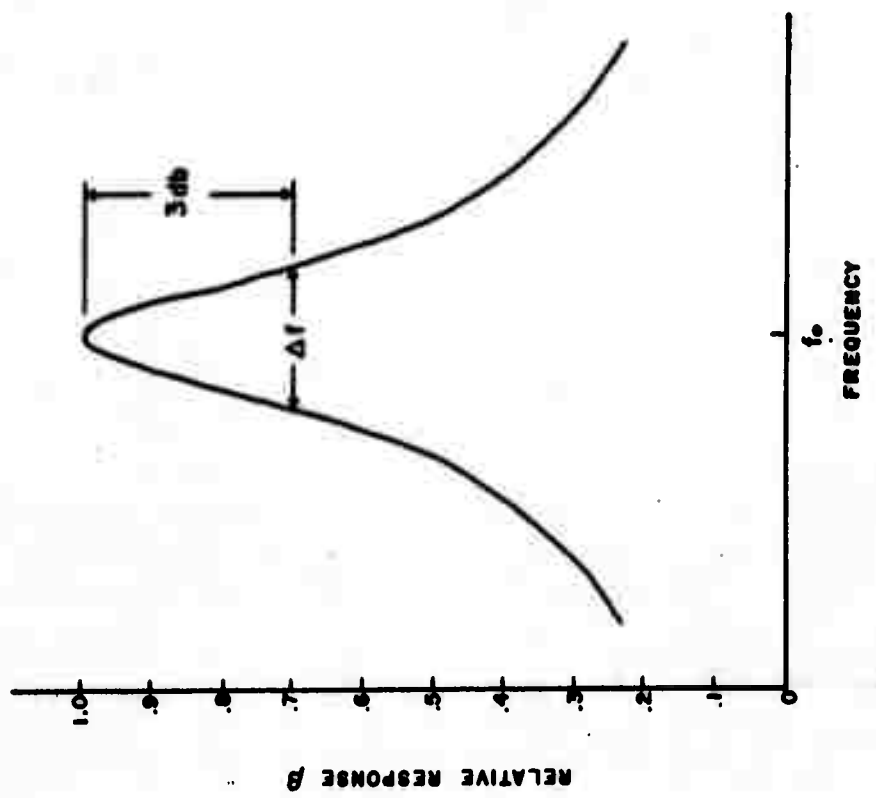
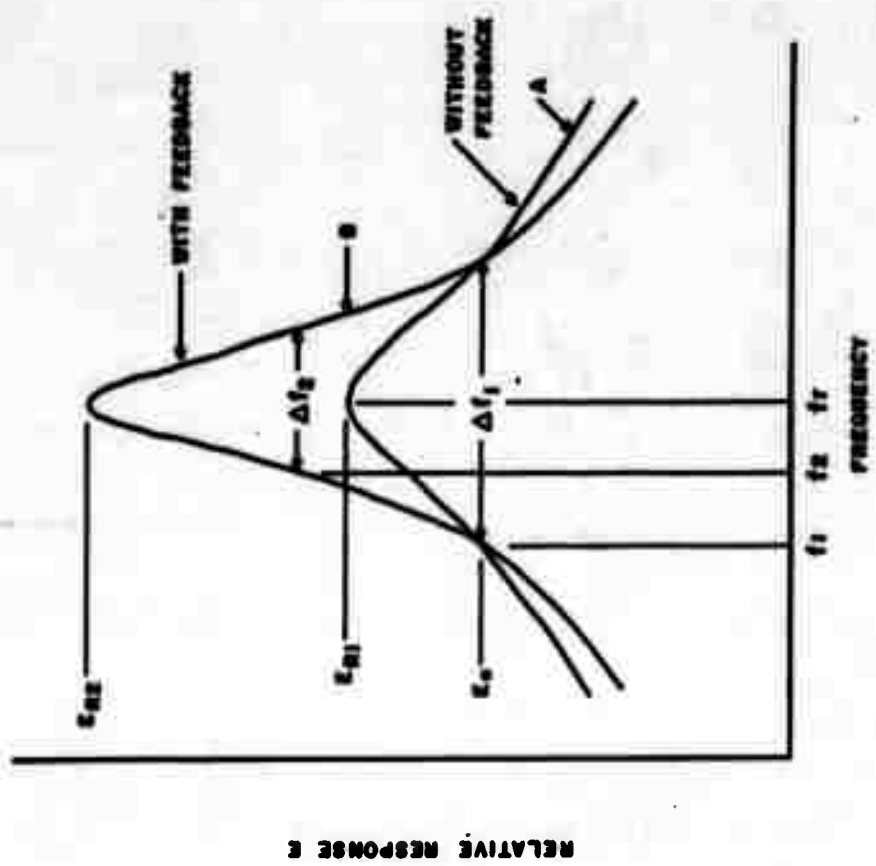
BASIC FEEDBACK LOOP

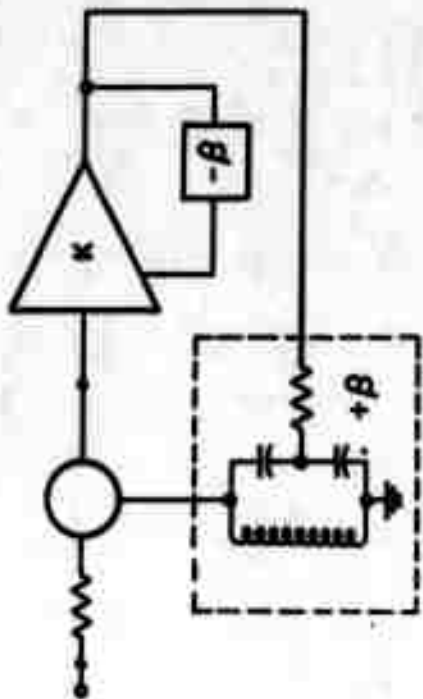
FIG. 8



FEEDBACK LOOP WITH RESONANT CIRCUIT AS β NETWORK

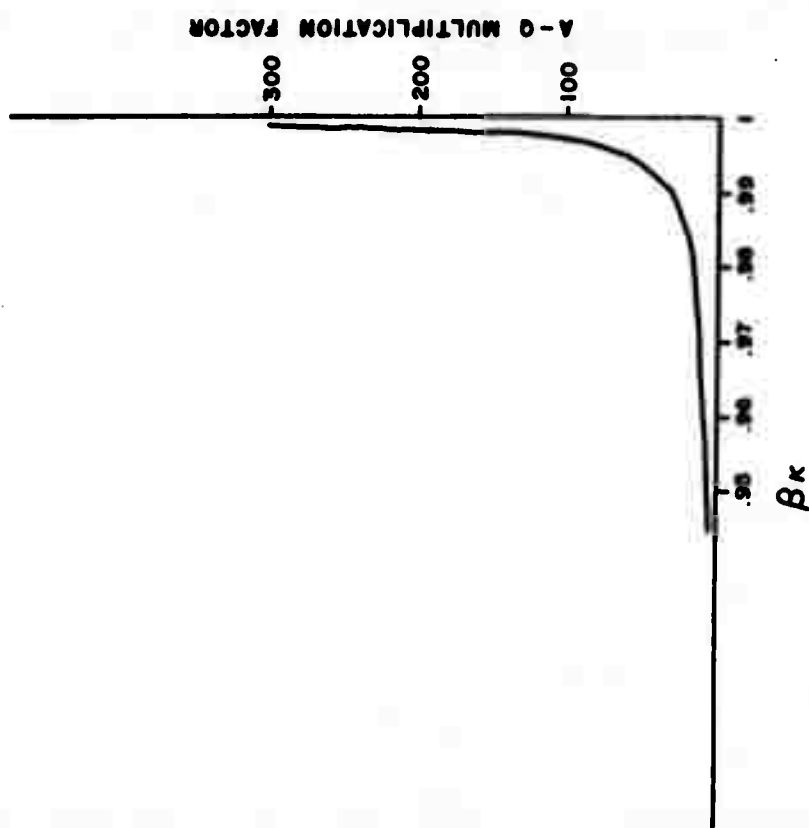
FIG. 9





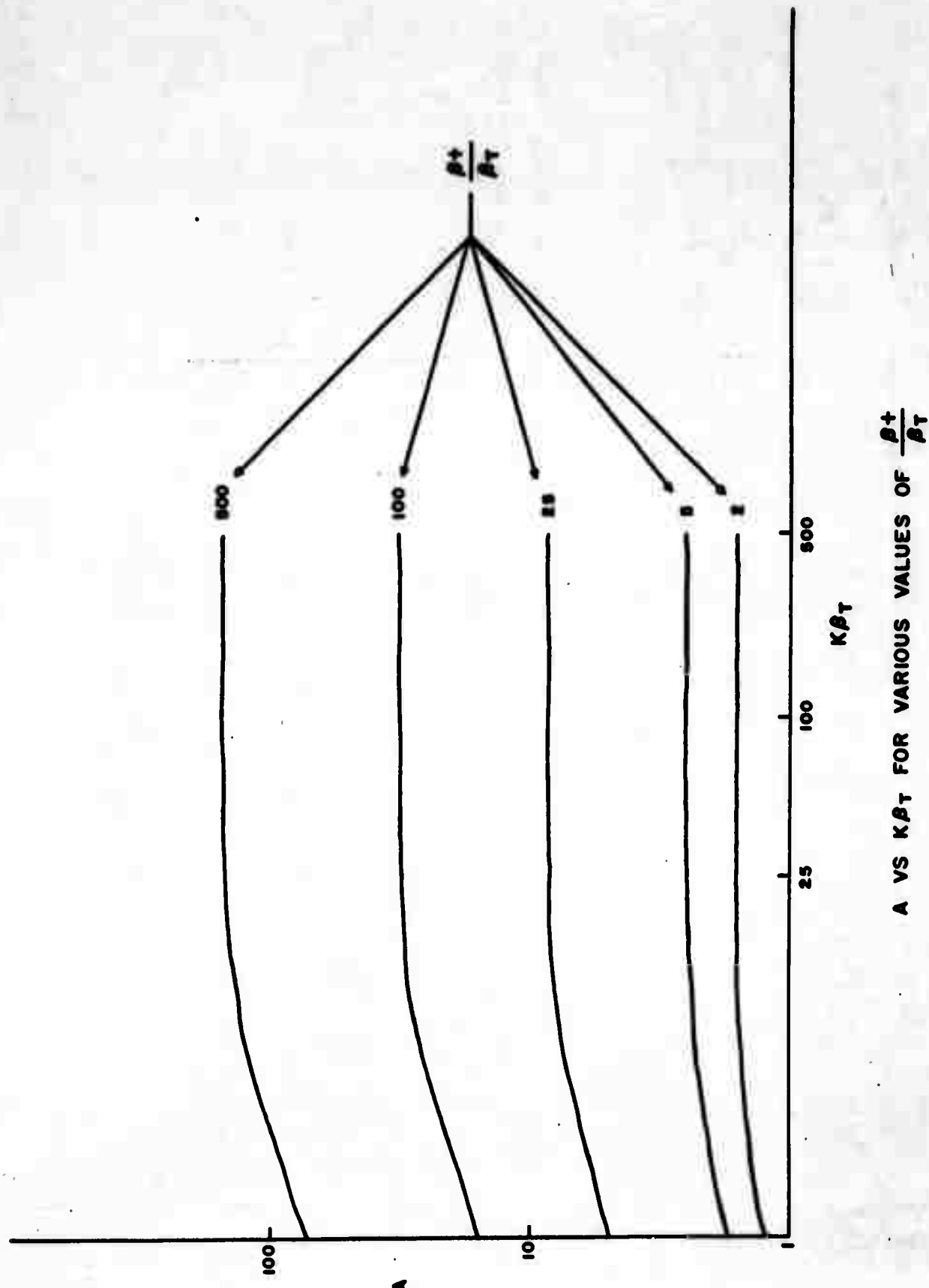
FEEDBACK LOOP WITH POSITIVE
AND NEGATIVE LOOPS

FIG. 13



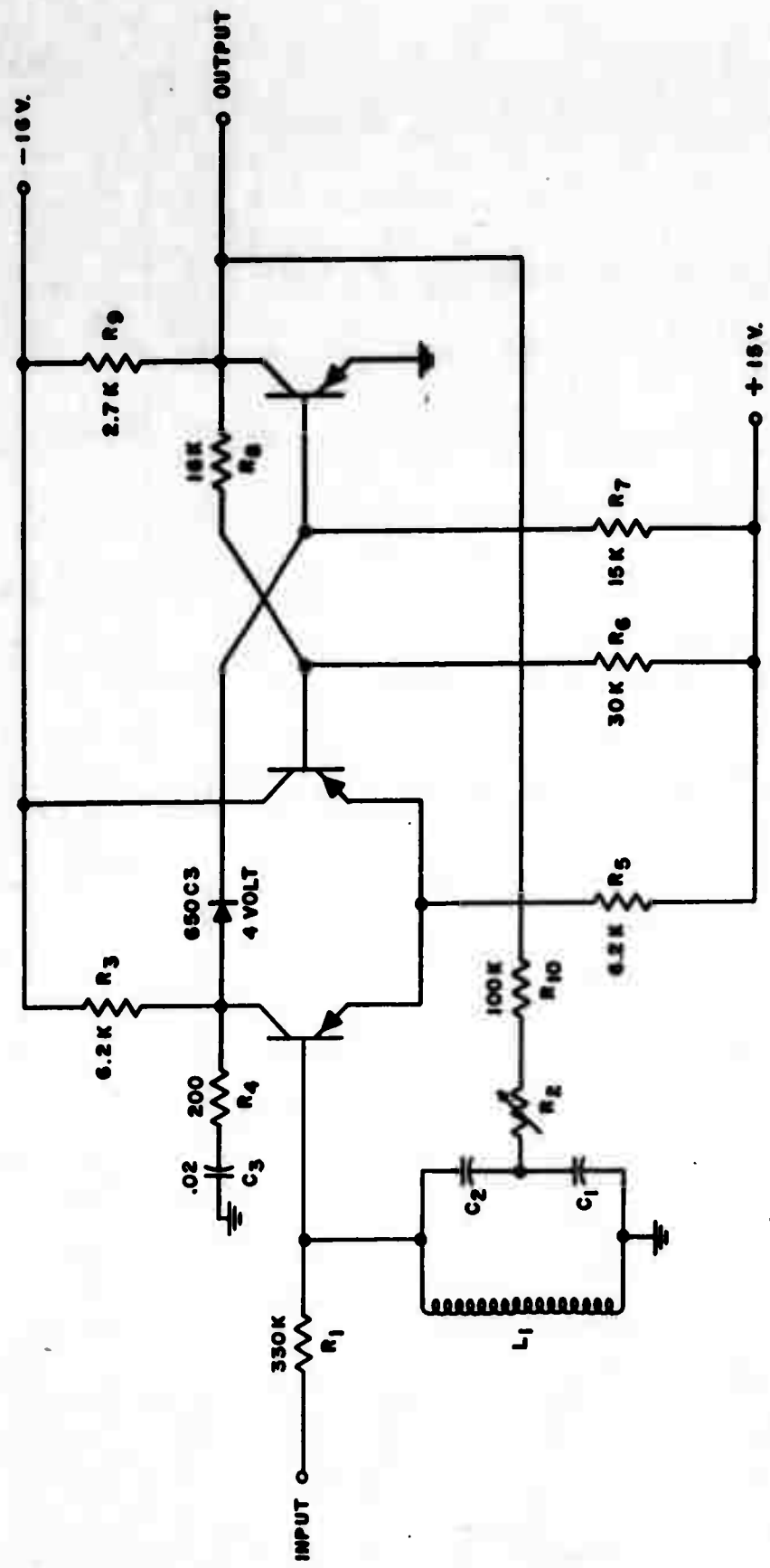
FEEDBACK VS Q MULTIPLICATION
FOR POSITIVE LOOP ONLY

FIG. 12



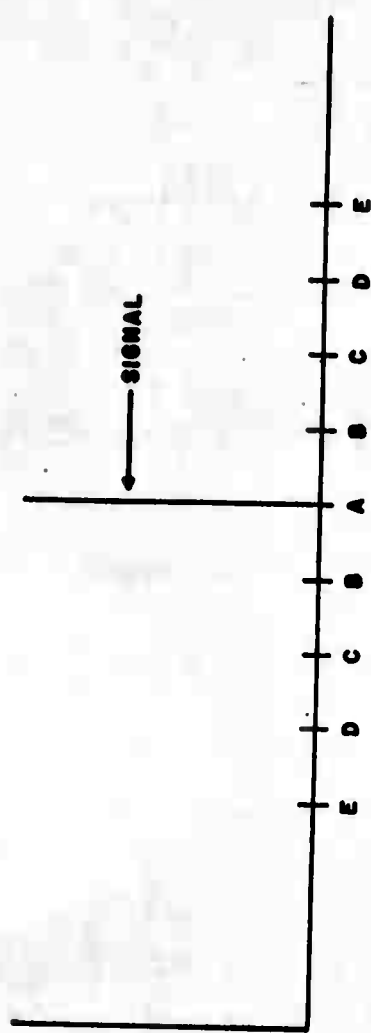
A VS $K\beta_T$ FOR VARIOUS VALUES OF $\frac{\beta^+}{\beta_T}$

FIG. 14



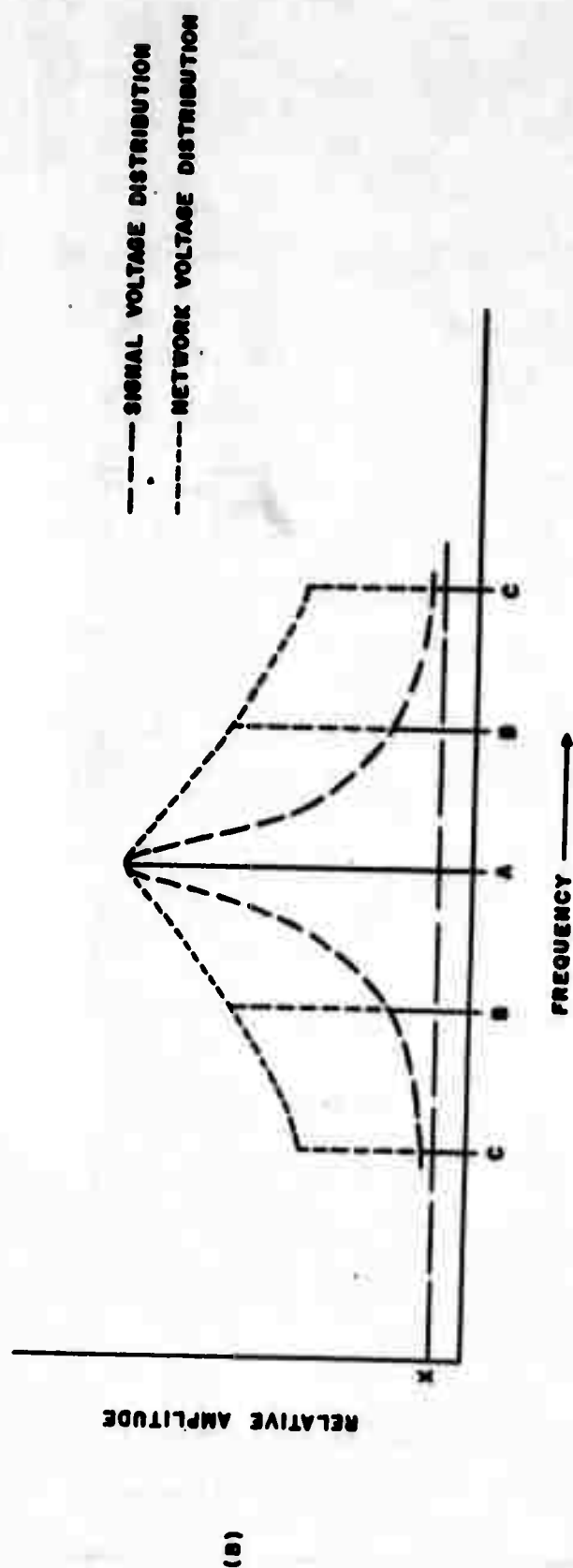
Q MULTIPLIER SCHEMATIC

FIG. 15



FILTER IDENTIFICATION AND LOCATION

(a)

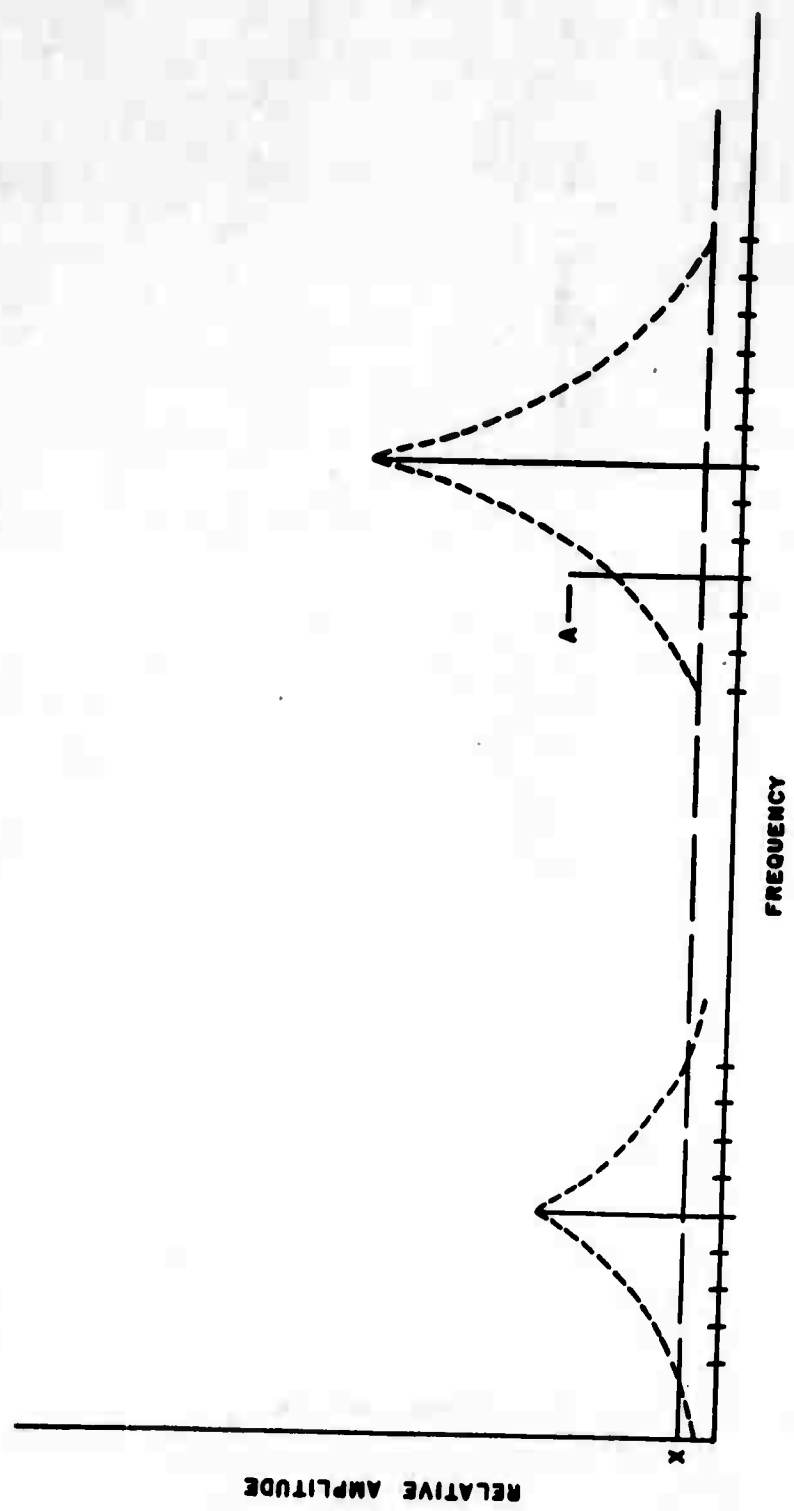


— SIGNAL VOLTAGE DISTRIBUTION
- - - NETWORK VOLTAGE DISTRIBUTION

(b)

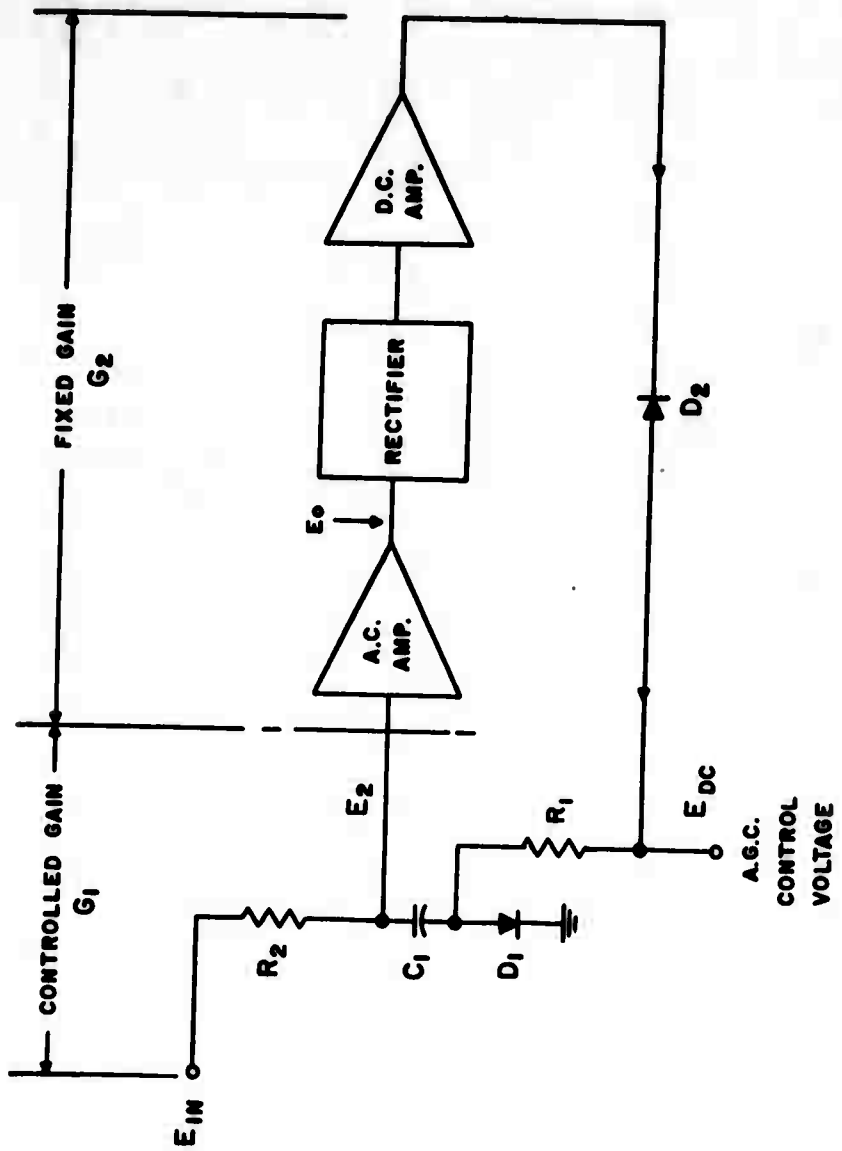
SIGNAL AND NETWORK VOLTAGE DISTRIBUTION VS FREQUENCY

FIG. 16



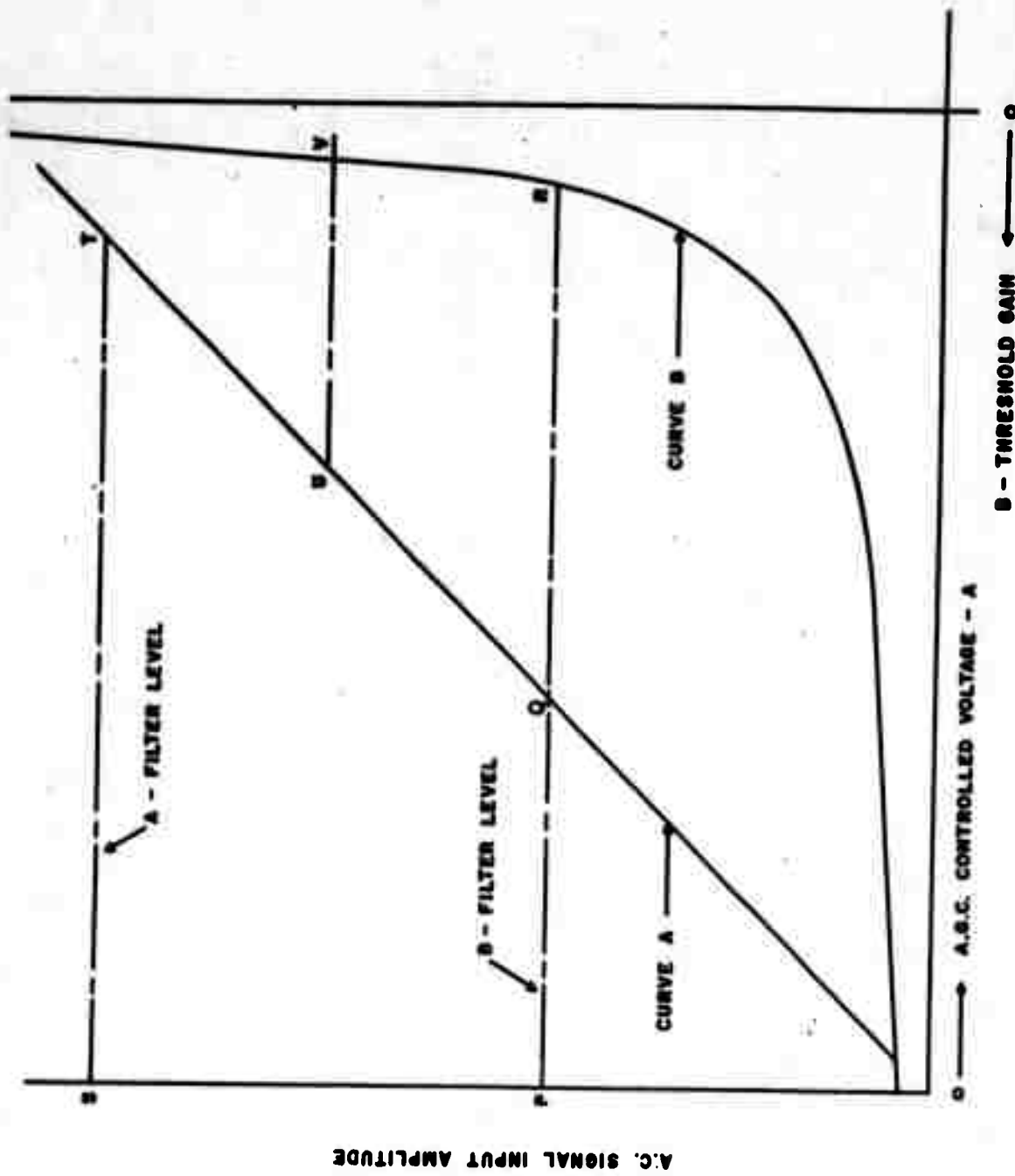
NETWORK VOLTAGE DISTRIBUTION FOR DIFFERENT AMPLITUDES VS FREQUENCY

FIG. 17



AMPLIFIED DELAYED A.G.C.

FIG. 18



A.G.C. CONTROL VOLTAGE AND THRESHOLD GAIN VS A.C. SIGNAL INPUT

FIG. 19

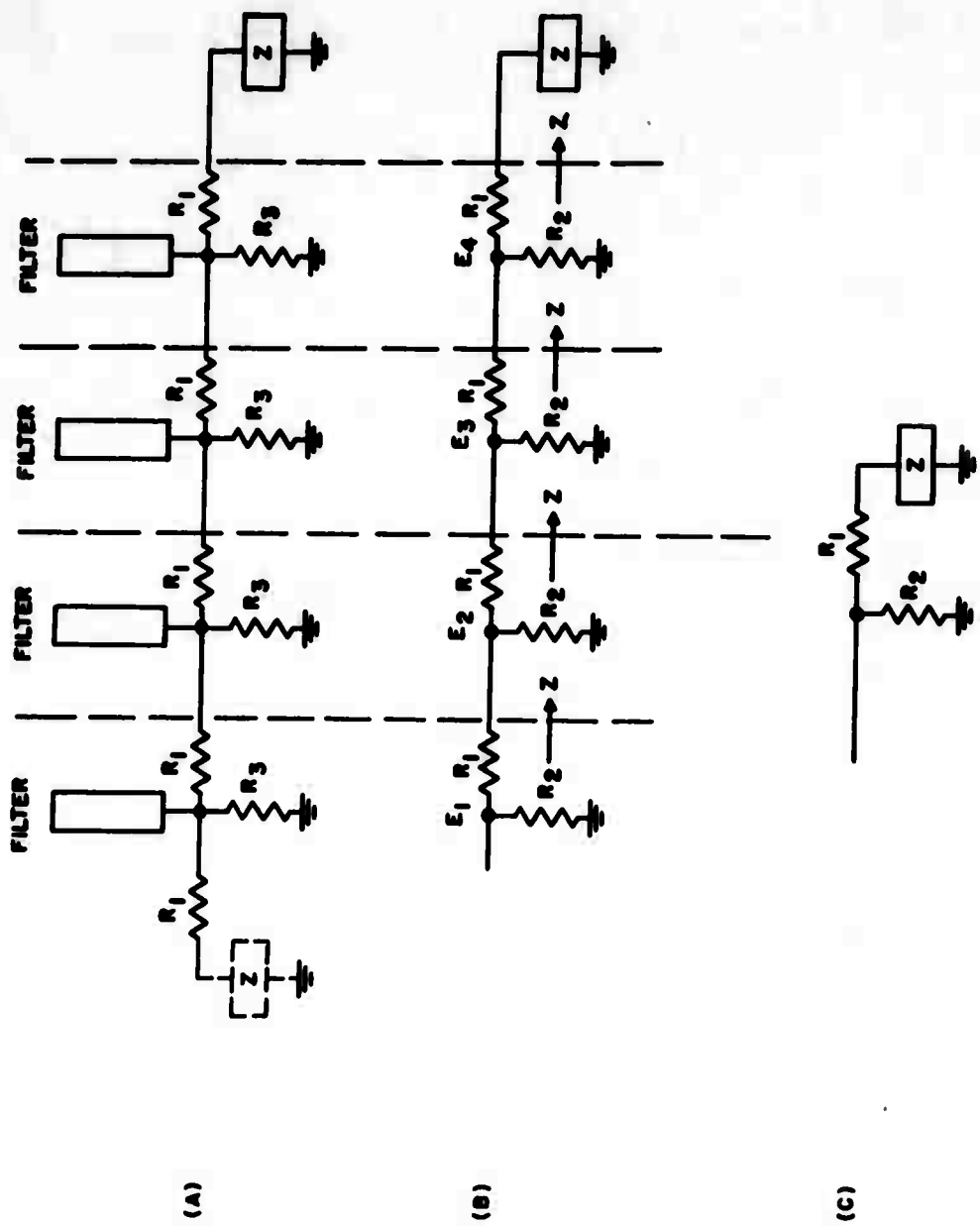
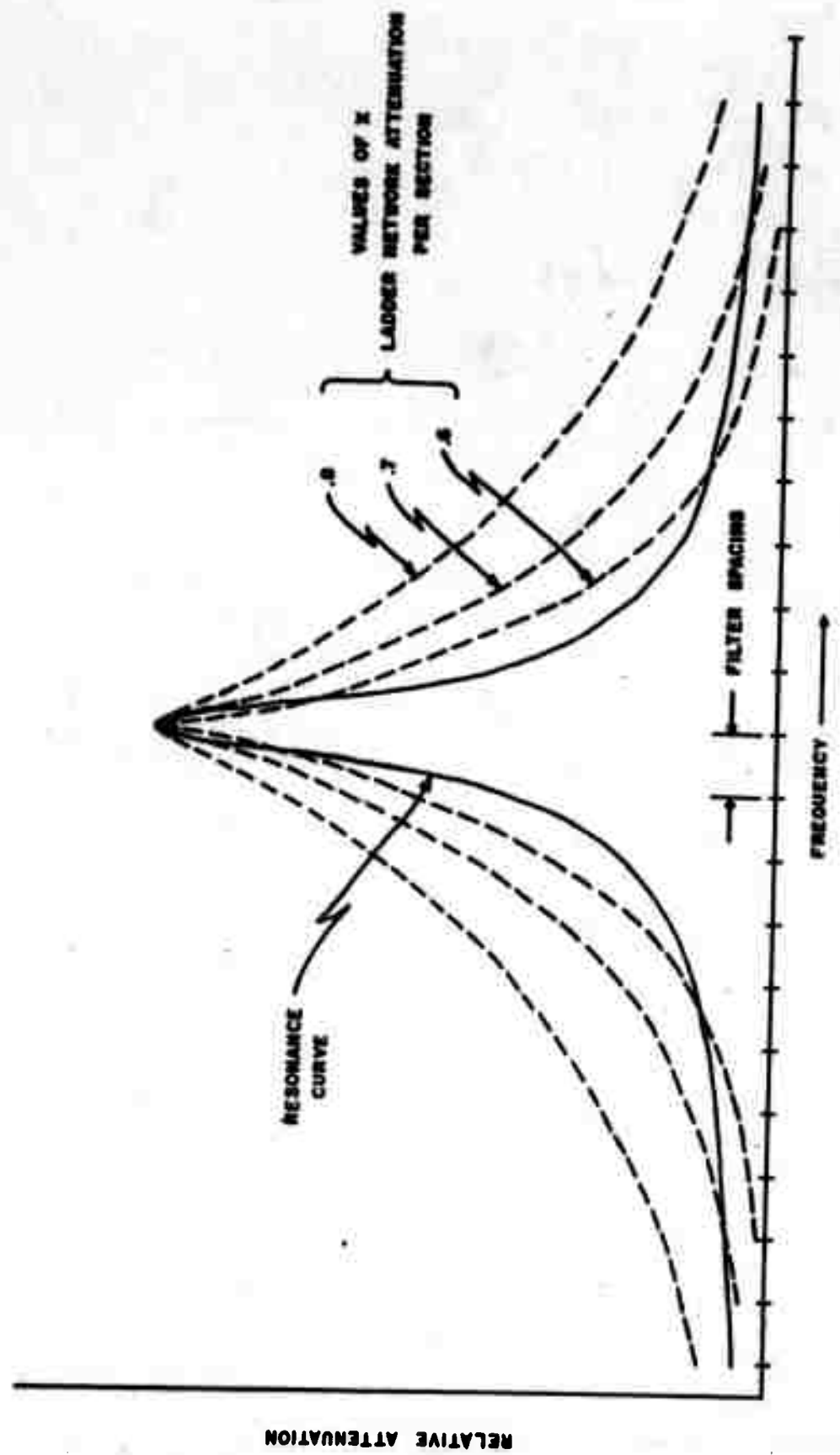
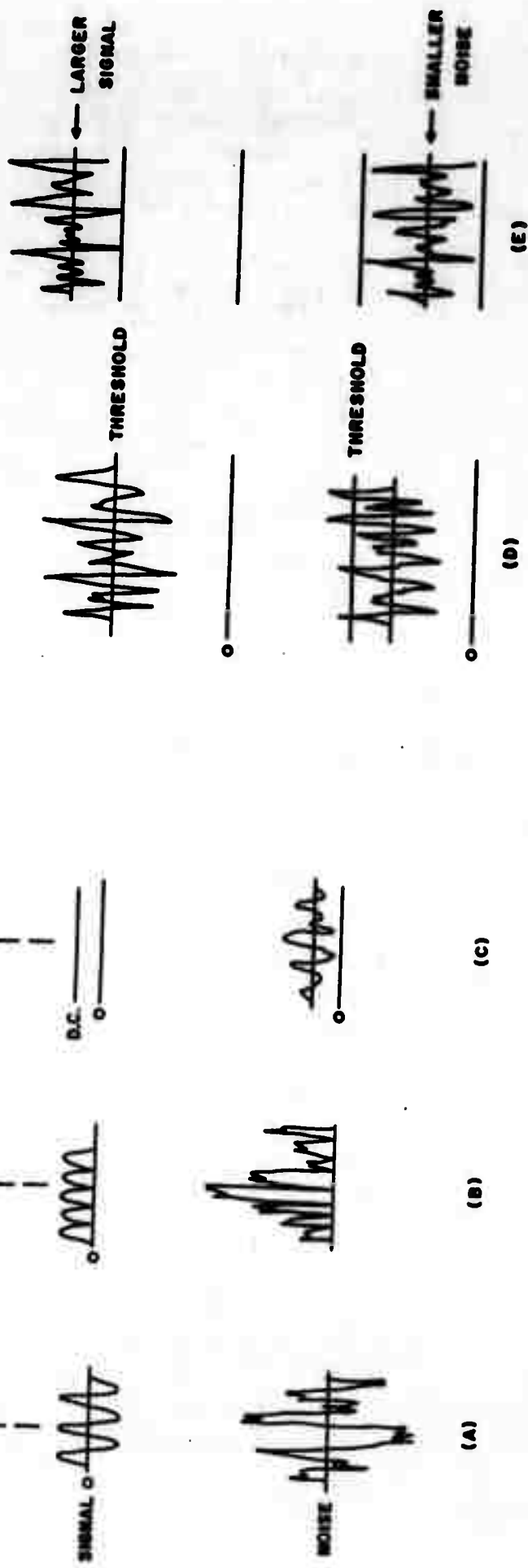
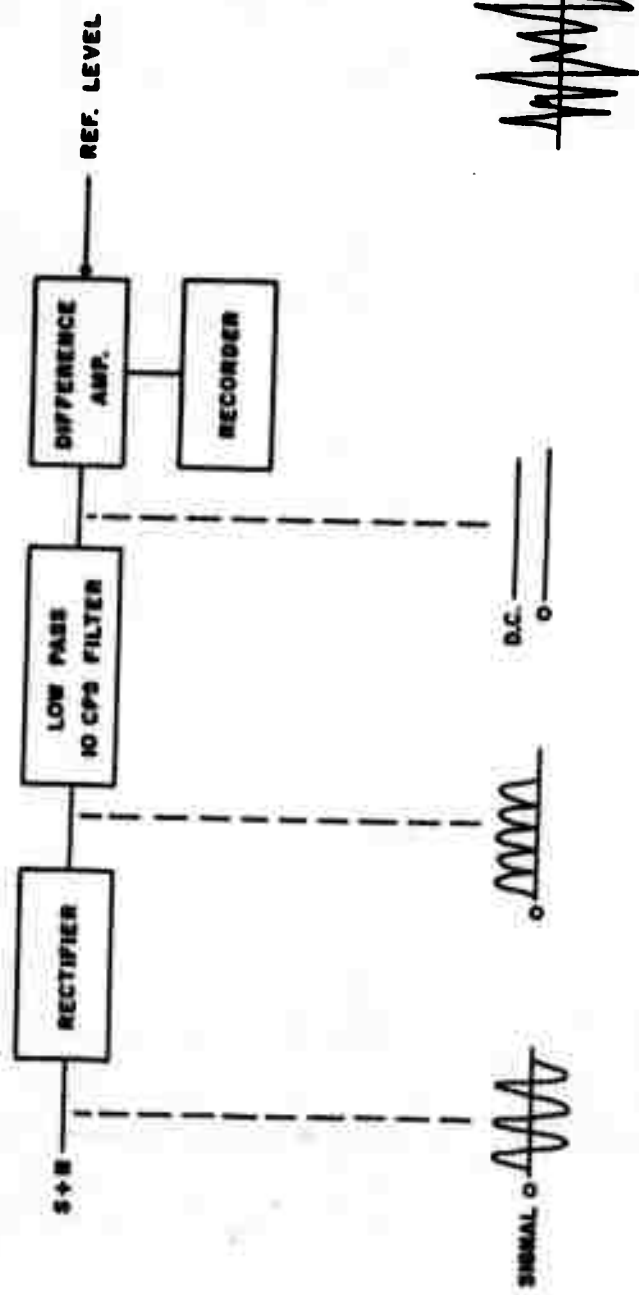


FIG. 20
LADDER NETWORK



LADDER NETWORK ATTENUATION VS FILTER SPACING

FIG. 21



THRESHOLD CIRCUIT BLOCK DIAGRAM AND VOLTAGE LEVELS

FIG. 22

OPTIMUM NOISE LEVEL
FOR
MAXIMUM SENSITIVITY
VARIABLE NOISE
VS
SIGNAL LEVEL

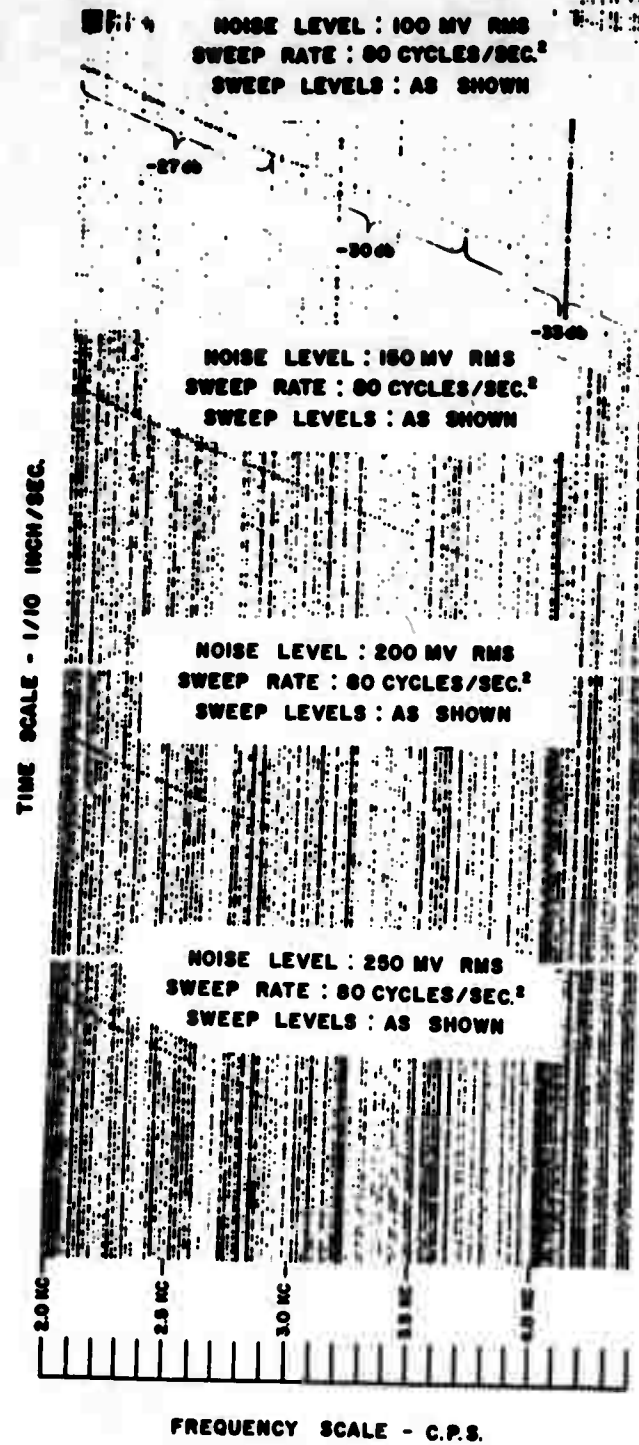


FIG. 23

SENSITIVITY CHART

VARIABLE NOISE AND SIGNAL LEVEL TO
DETERMINE OPTIMUM SENSITIVITY

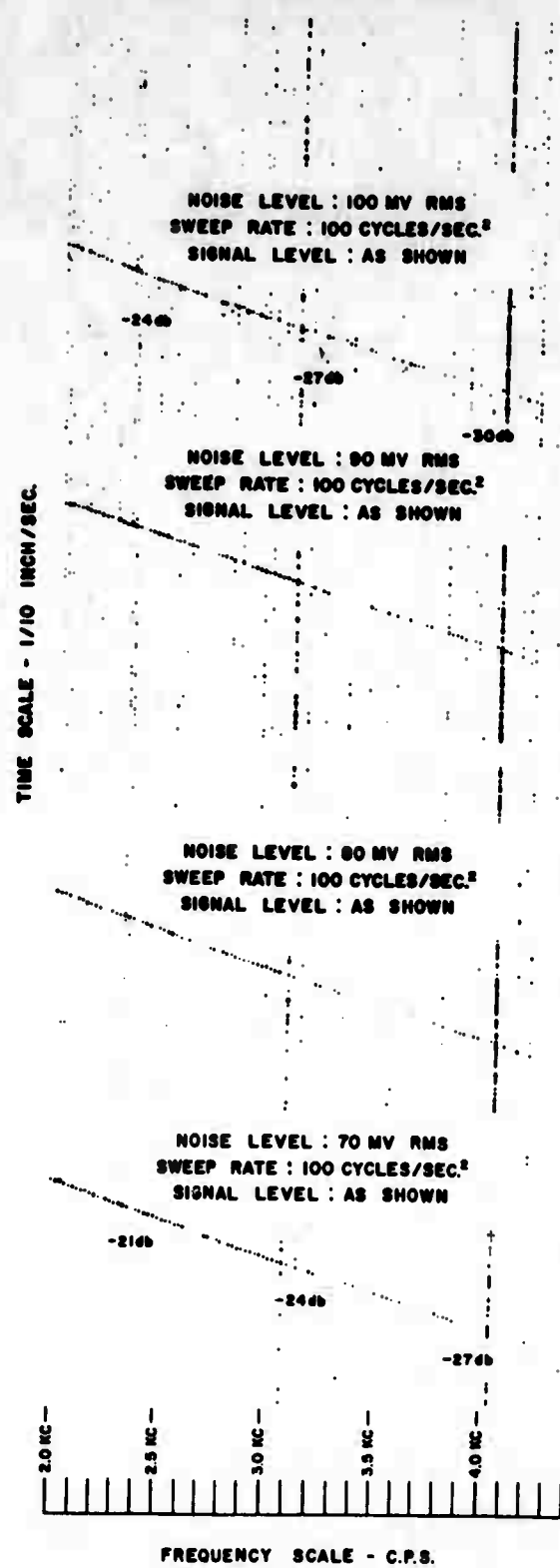


FIG. 24

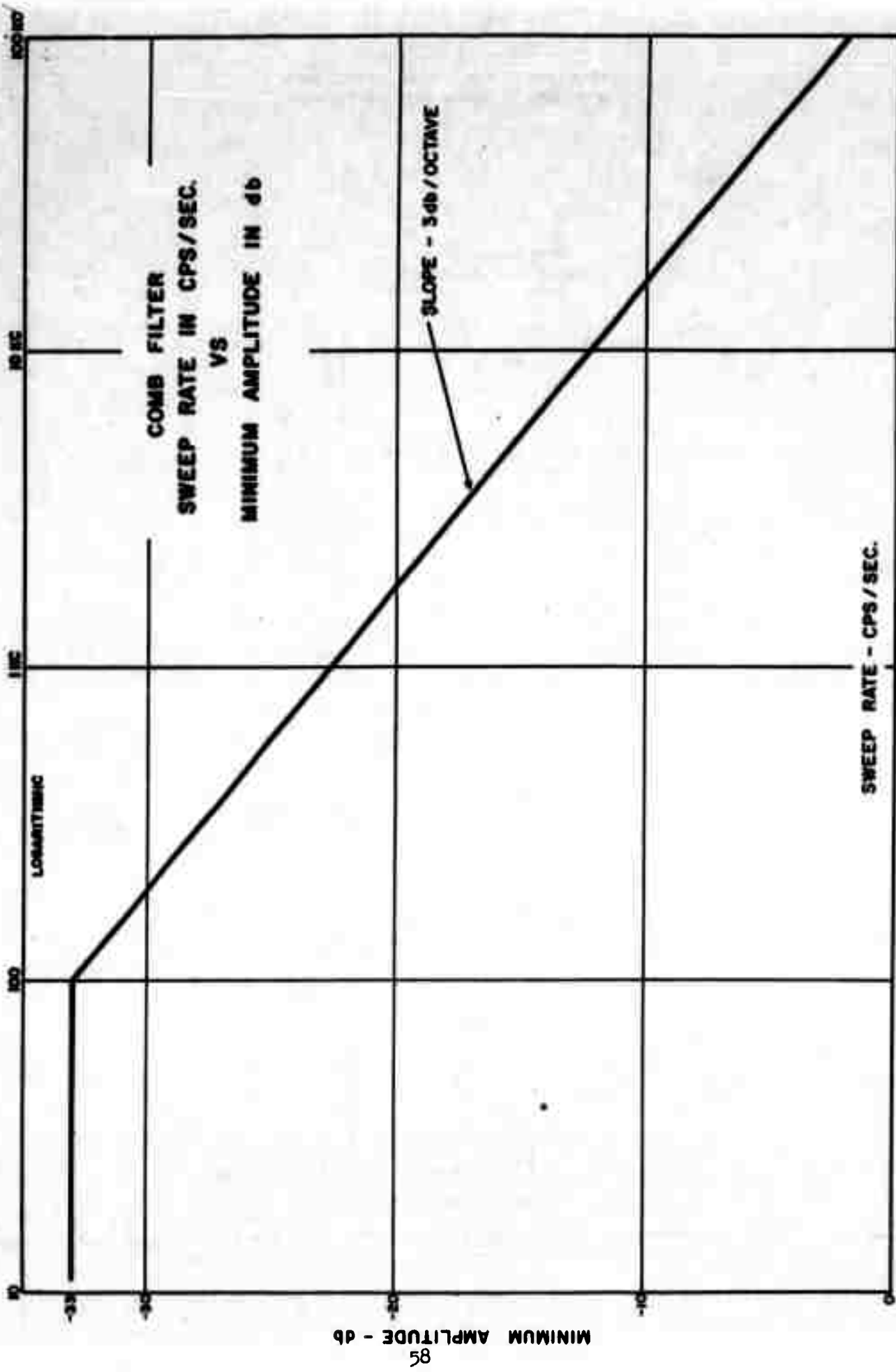


FIG. 25

DYNAMIC RANGE CHART
RANGE OF MAXIMUM TO MINIMUM LEVELS
GIVING SINGLE PEN OPERATION

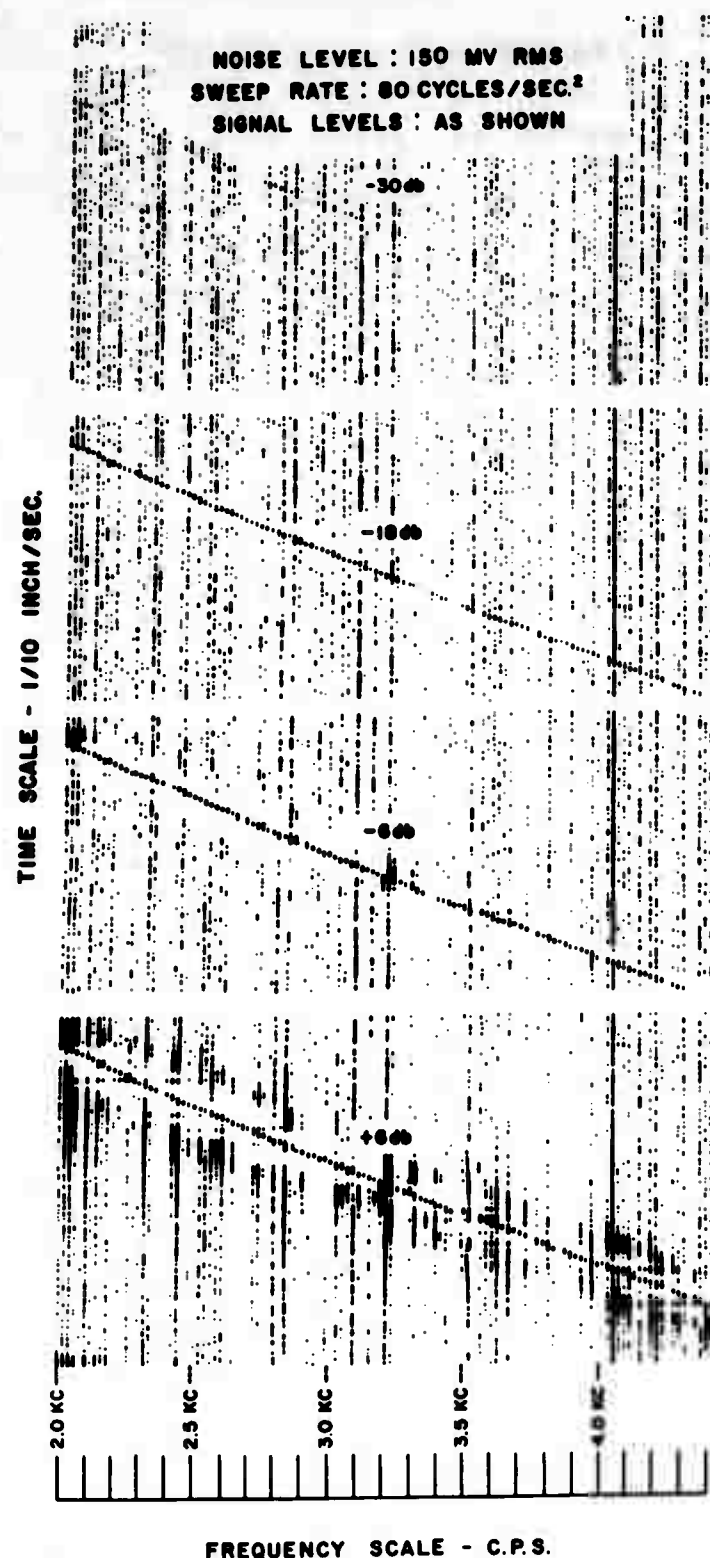


FIG. 26

AGC ACTION CHART
LARGE AMPLITUDE FIXED FREQUENCY SIGNAL
VS
SWEEP SIGNAL LEVEL

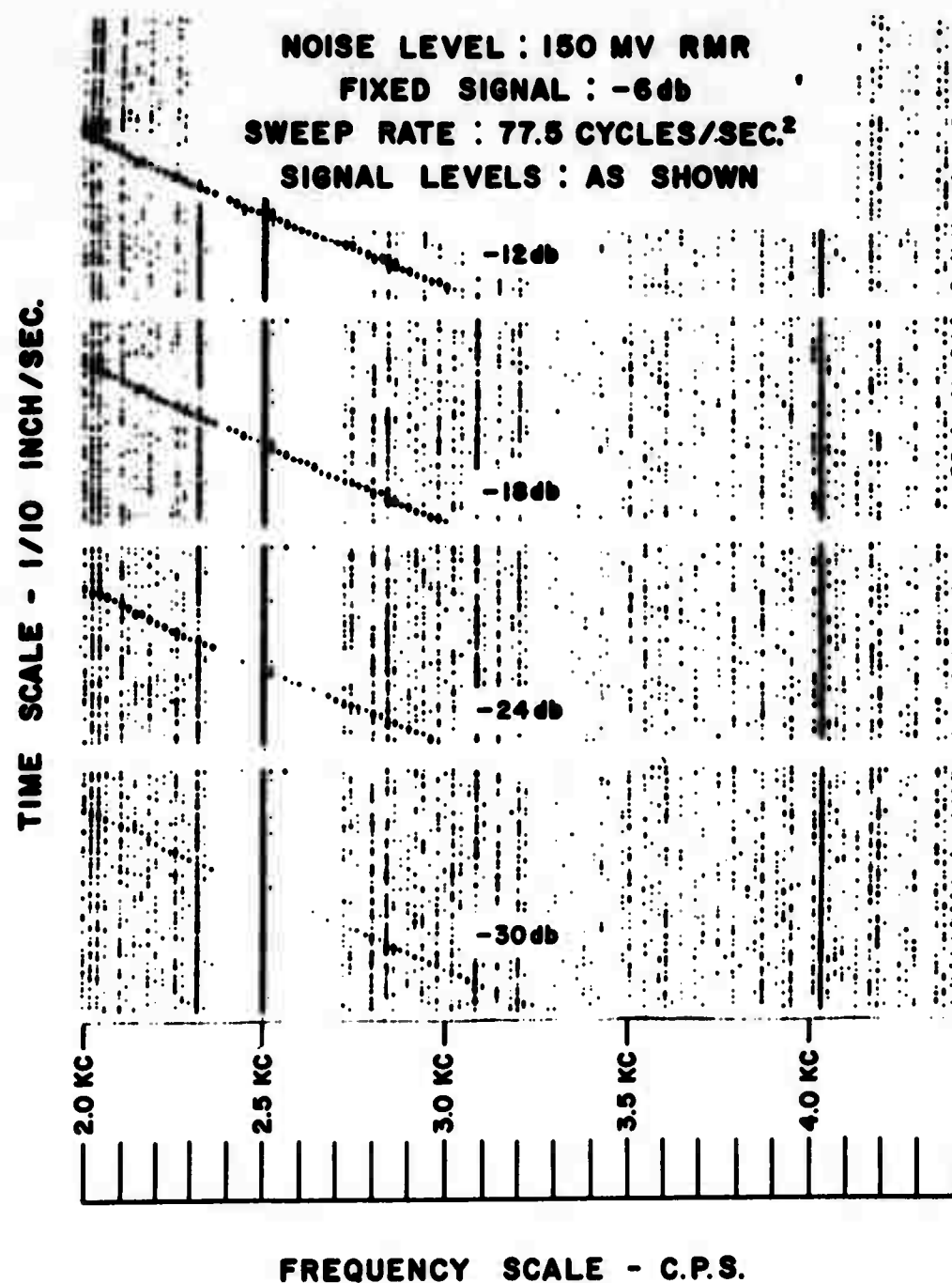


FIG. 27

TWO CROSSING SIGNALS
WITH VARIABLE SWEEP RATES

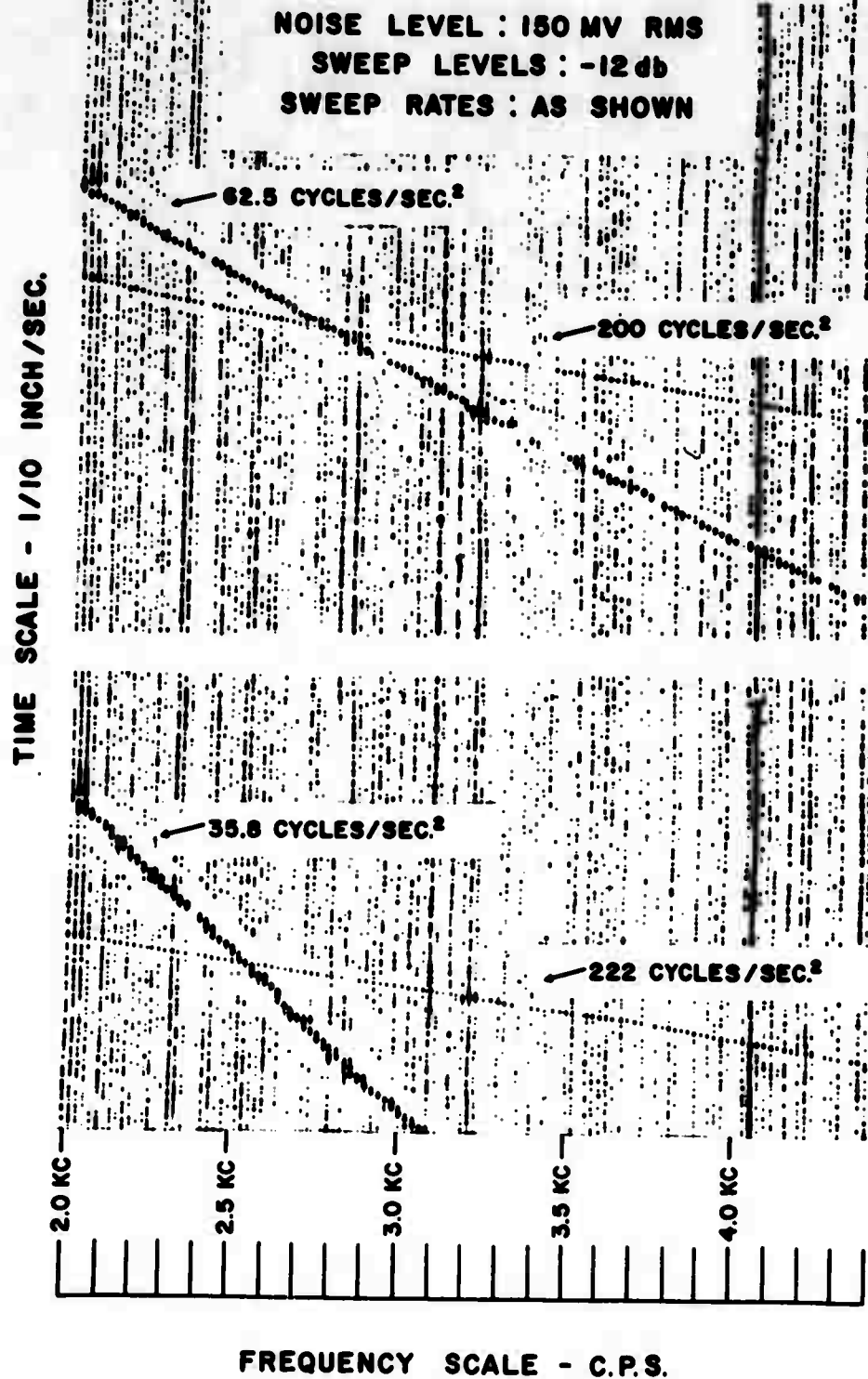


FIG. 28

60 DELTA REV. 124
NORTH - CENTER - SOUTH ANTENNAS
NORTH - SOUTH PASS

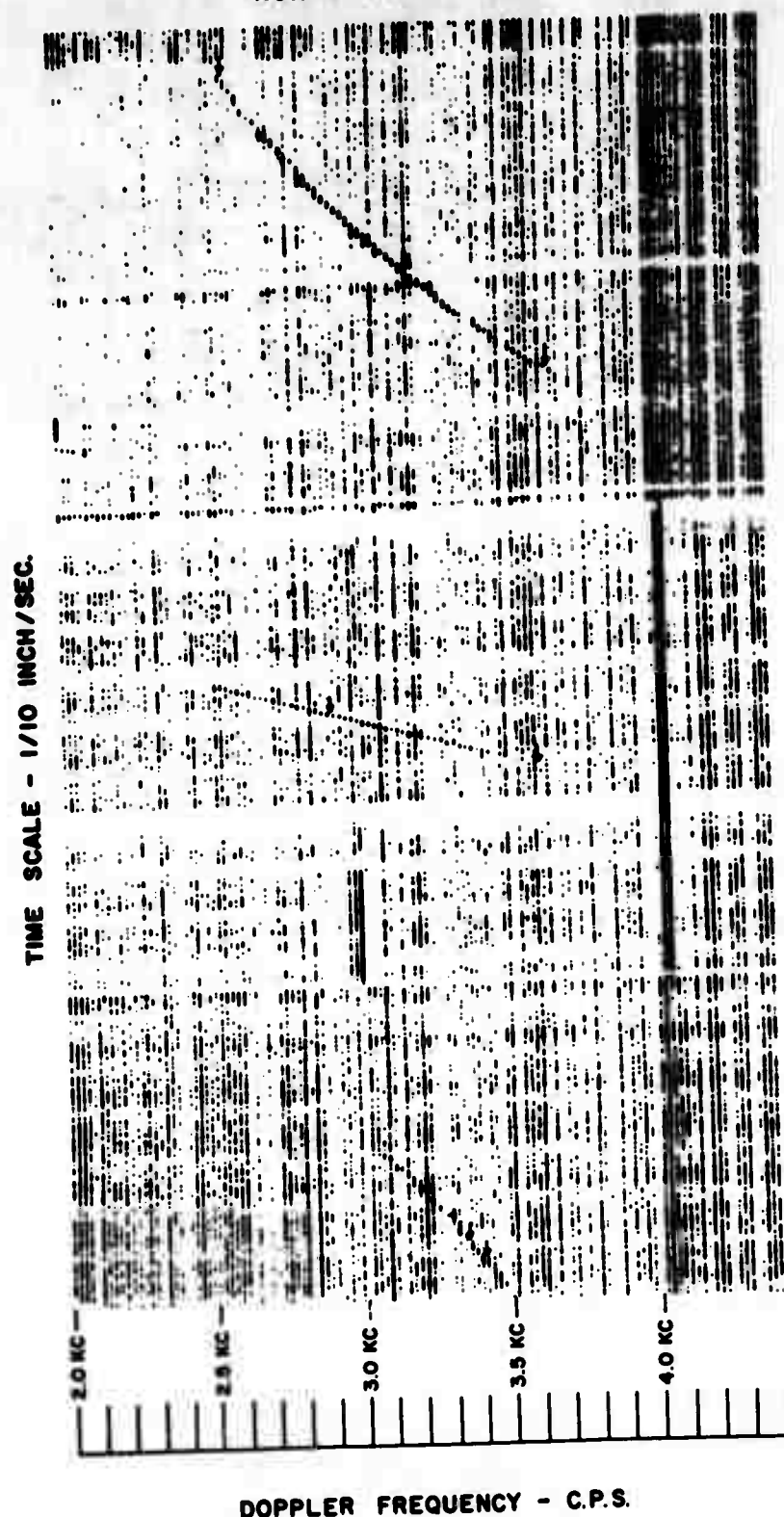
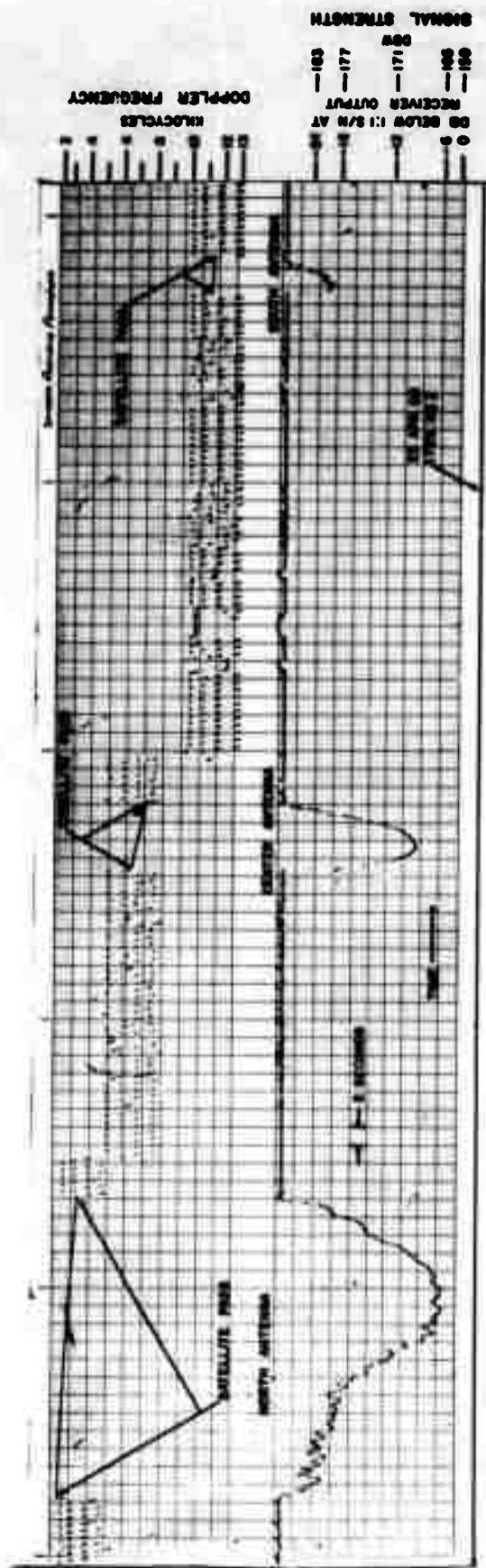


FIG. 29A



ARPA - BRL DOPPLER RECORD OF
60 DELTA REV. 124, FOREST CITY, ARKANSAS
MEASURED 1728:18 Z, PREDICTED 1729 Z
ALTITUDE 120 MILES, 350 MILES EAST FT. SILL
NORTH - CENTER - SOUTH ANTENNAS, NORTH - SOUTH PASS

FIG. 298

60 DELTA REV. 140
NORTH - CENTER - SOUTH ANTENNAS
NORTH - SOUTH PASS

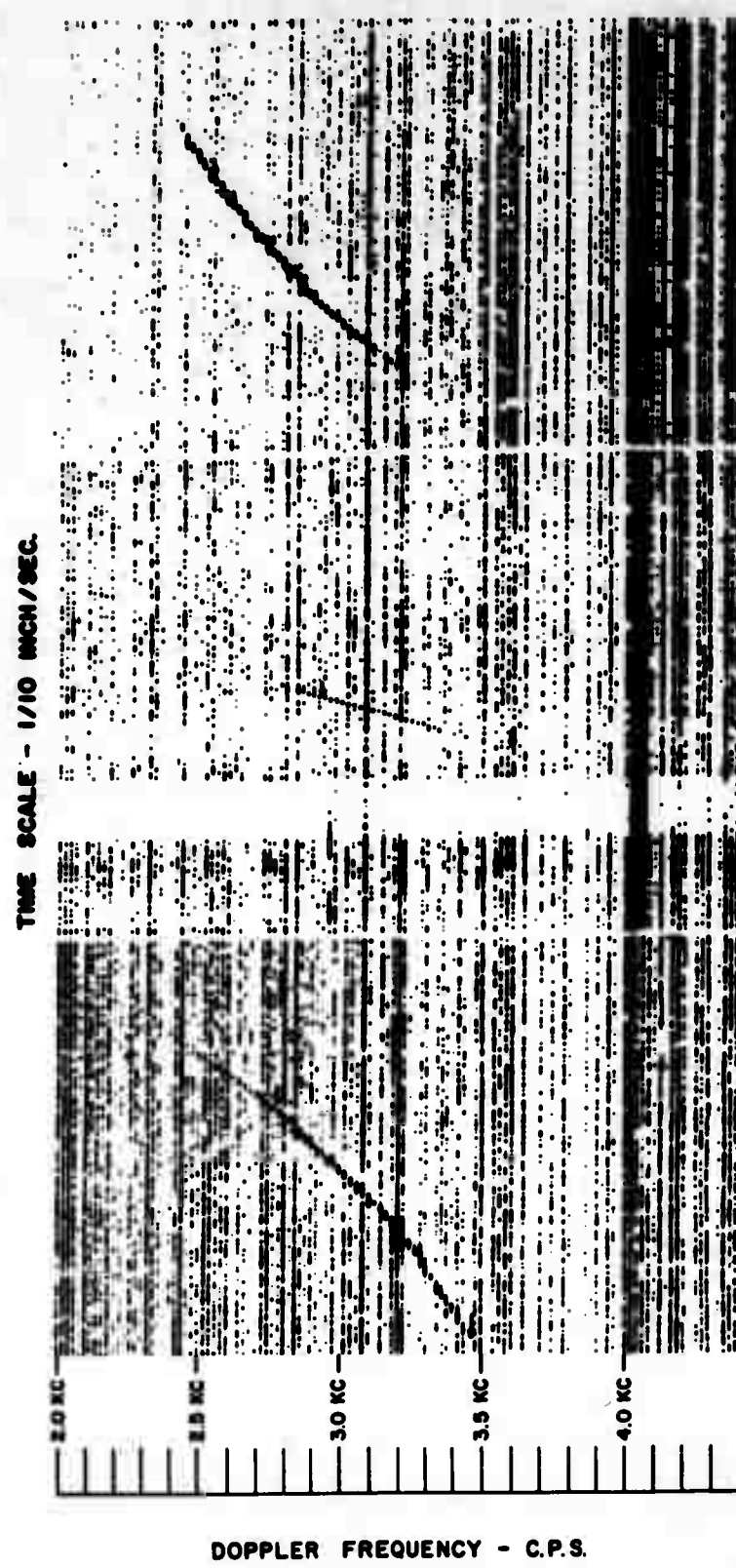
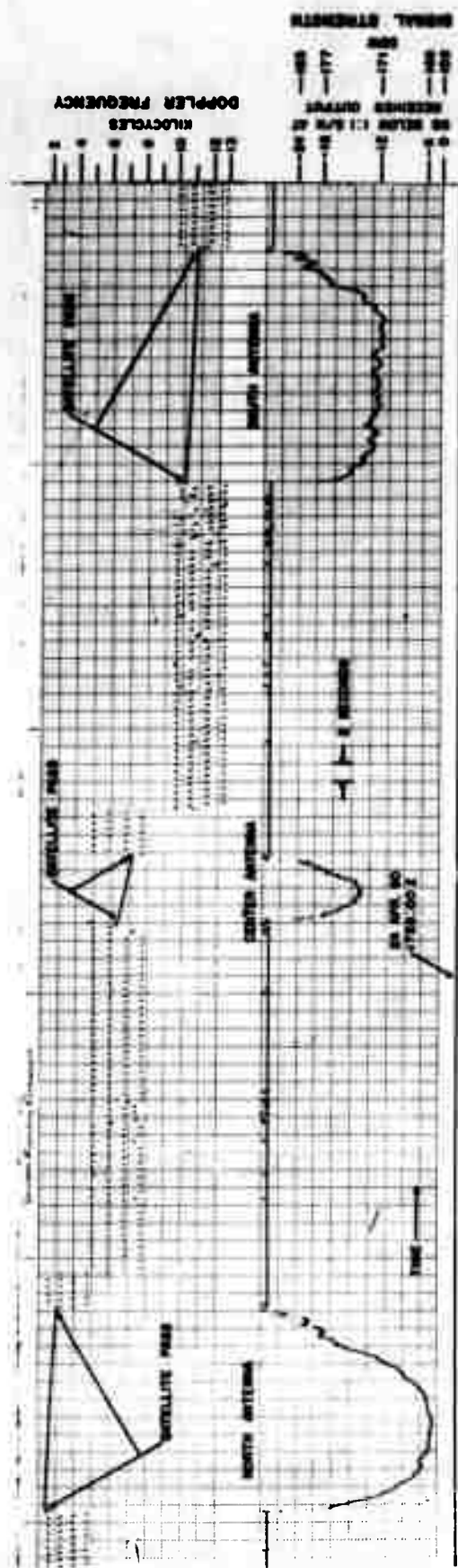


FIG. 30A



ARPA - BRL DOPPLER RECORD OF
60 DELTA REV 140, FOREST CITY, ARKANSAS
MEASURED 1728:06 Z. PREDICTED 1732:02
ALITUDE 116 MILES, 320 MILES EAST FT. SILL
NORTH - CENTER - SOUTH ANTENNAS, NORTH - SOUTH PASS

FIG. 308

60 DELTA REV. 156
NORTH - CENTER - SOUTH ANTENNAS
NORTH - SOUTH PASS

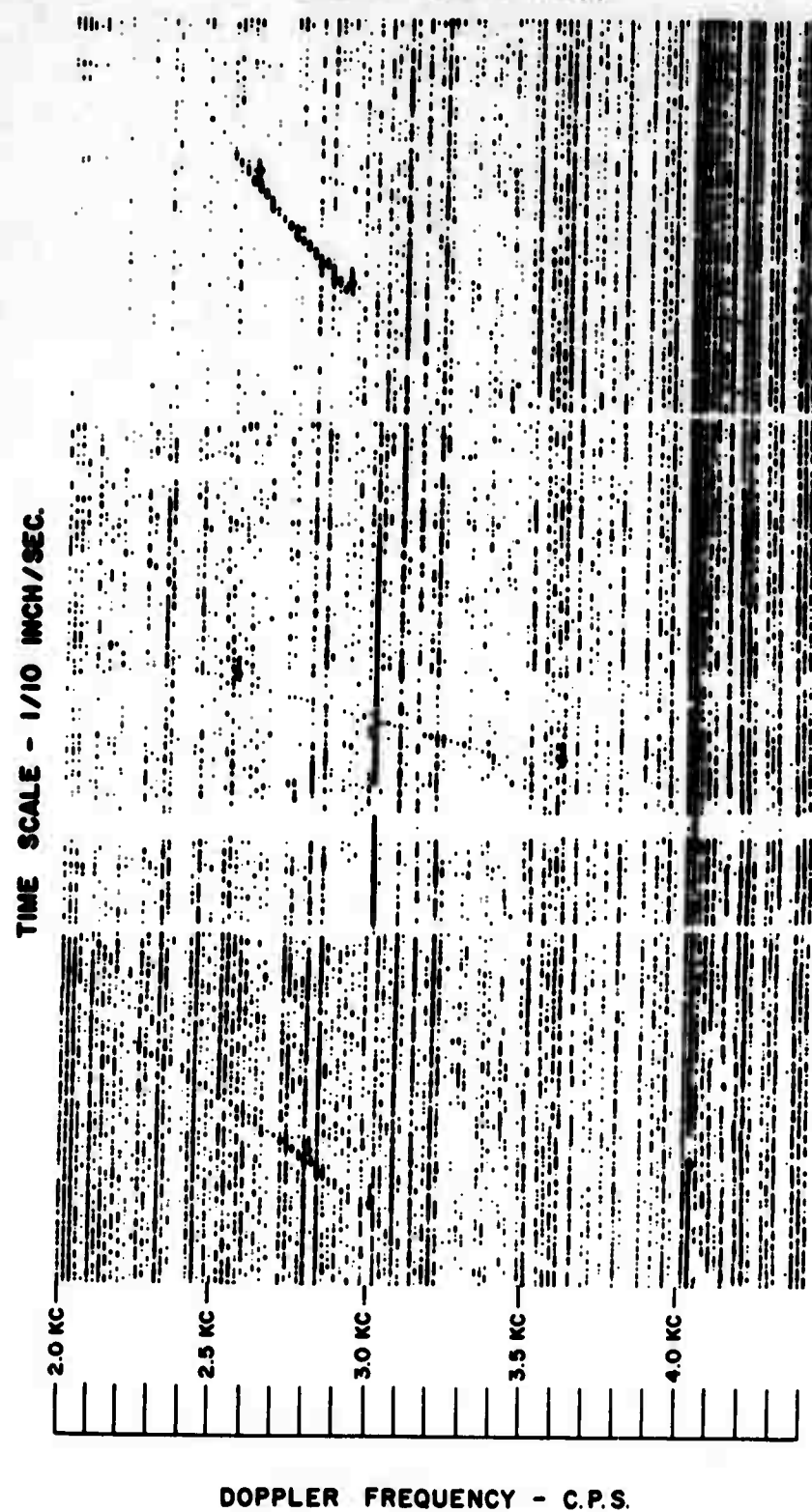
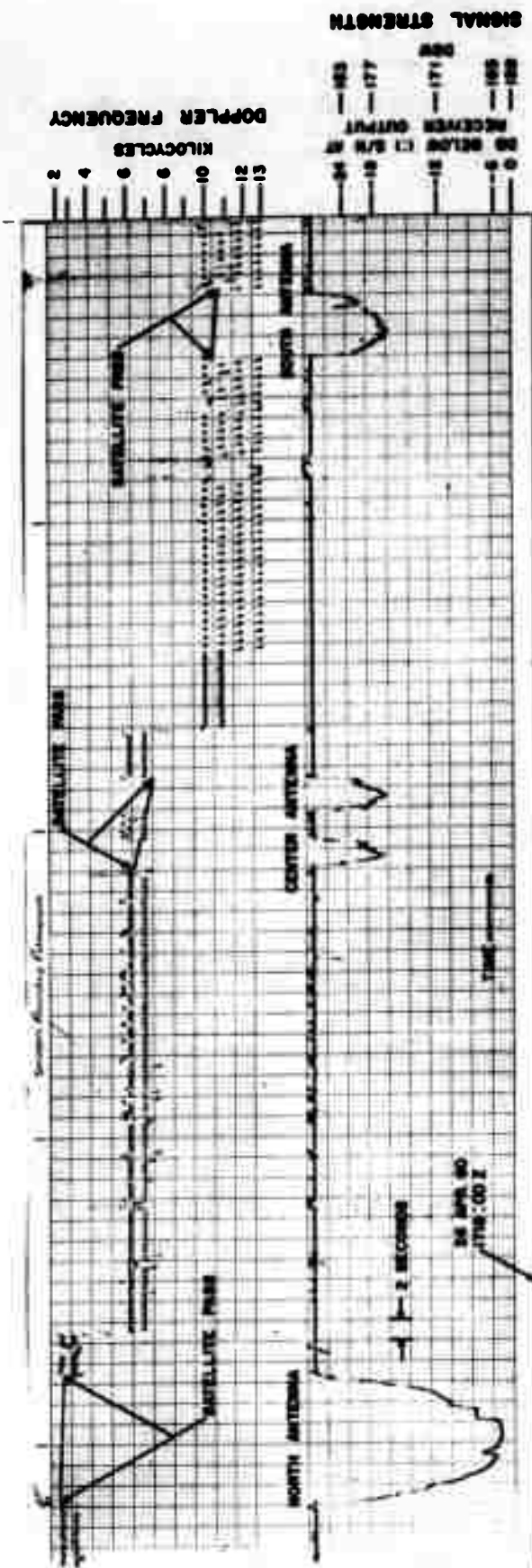


FIG. 31A



ANPA - BRL DOPLOC DOPPLER RECORD OF
60 DELTA REV. 166, FORREST CITY, ARKANSAS
MEASURED 1710:40 Z, PREDICTED 1725 Z
ALTITUDE 112 MILES, 143 MILES EAST FT. SILL
NORTH - CENTER - SOUTH ANTENNAS, NORTH - SOUTH PASS

FIG. 31B

60 DELTA REV. 165
NORTH - CENTER - SOUTH ANTENNAS
SOUTH - NORTH PASS

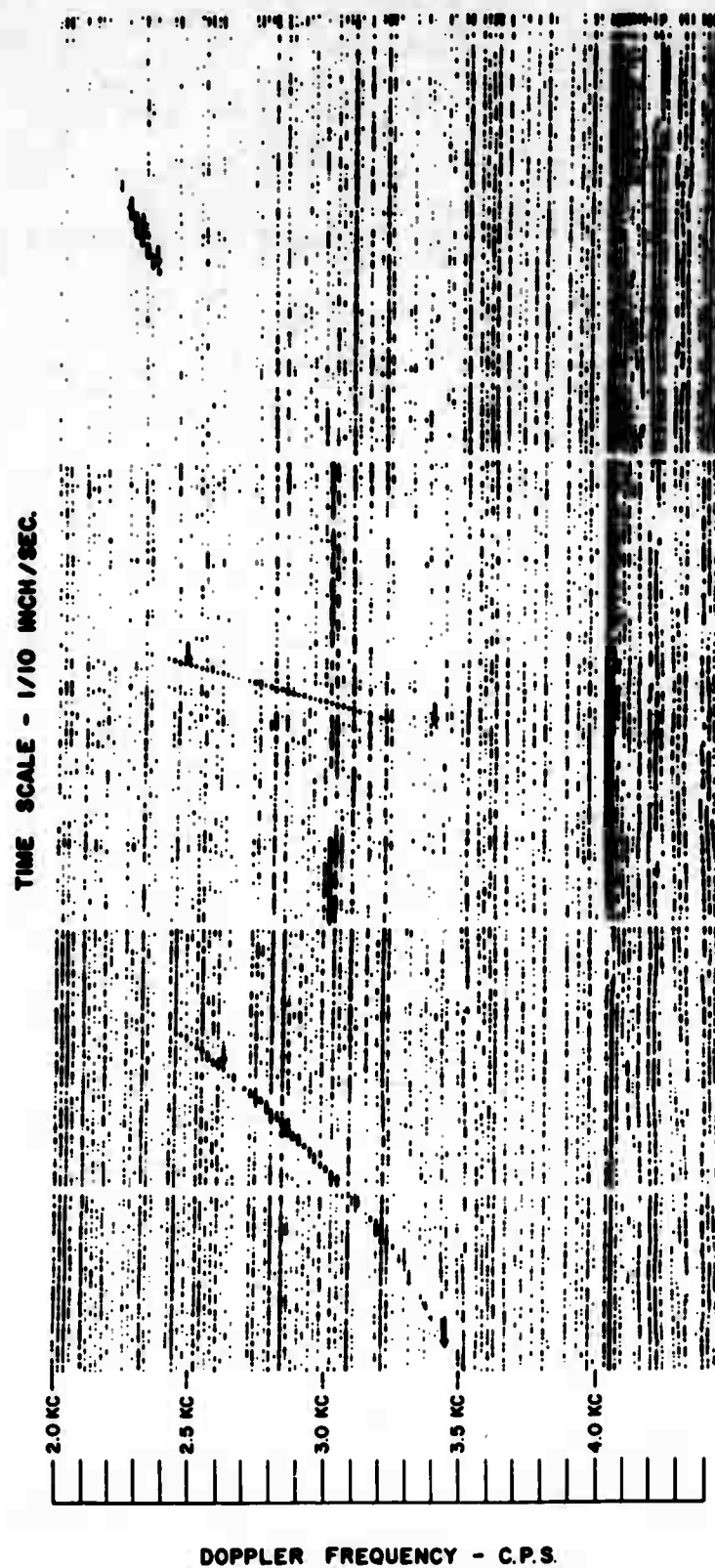
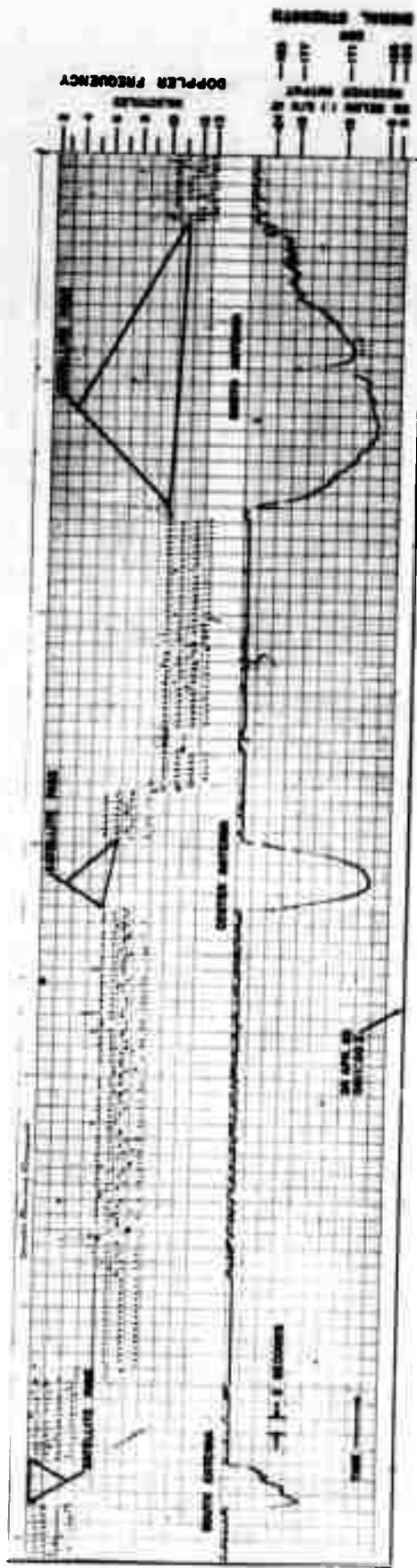


FIG. 32A



ANPA - BRL DOPPLER RECORD OF
60 MEGA CYCLES, FORREST CITY, ARKANSAS
MEASURED 061113Z, PREDICTED 0612
ALTITUDE 142 MILES, 30 MILES EAST FT. SILL
SOUTH - CENTER - NORTH ANTENNA, SOUTH - NORTH PLUS

FIG. 328

60 DELTA REV. 172
NORTH - CENTER - SOUTH ANTENNAS
NORTH - SOUTH PASS

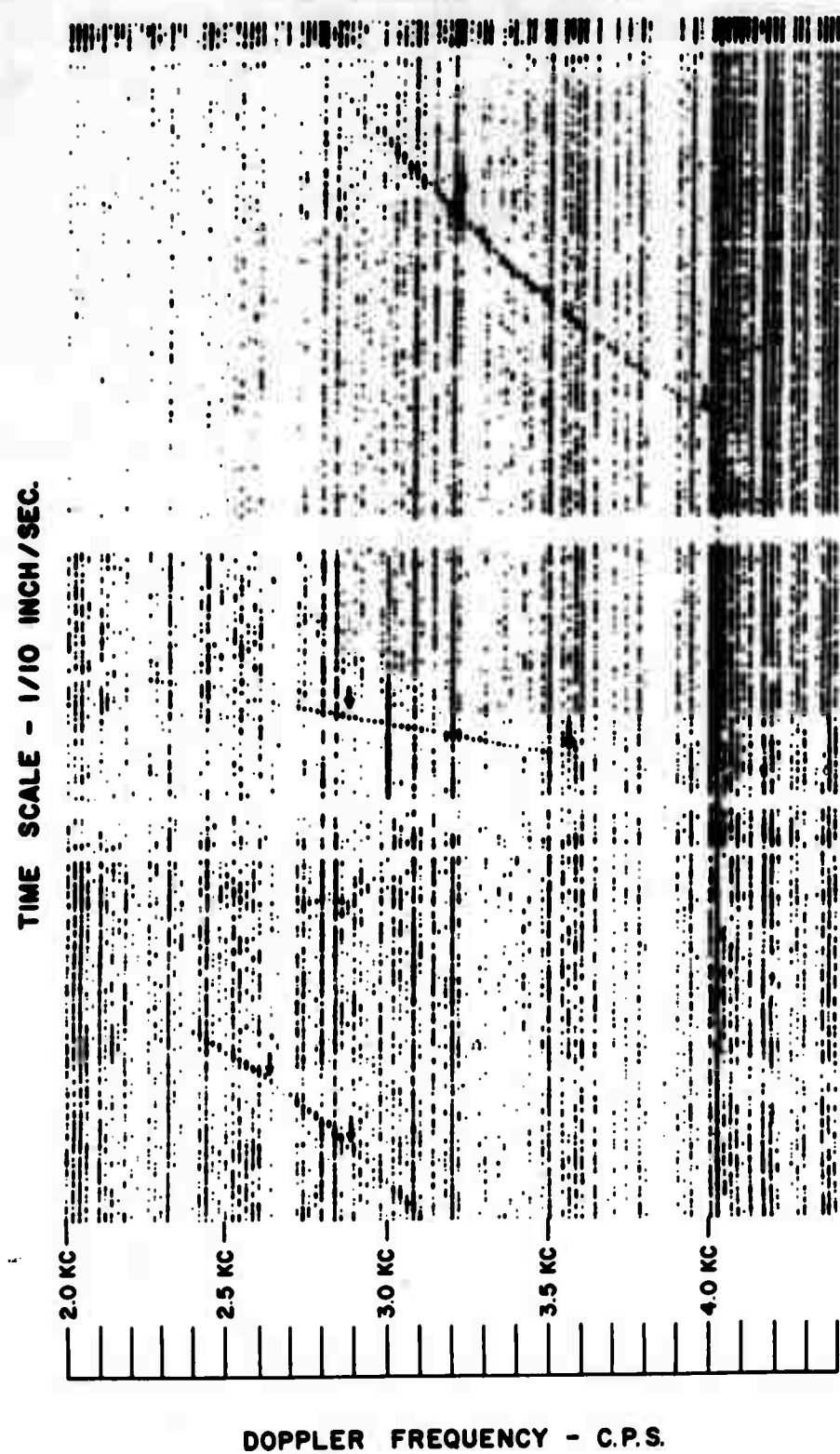
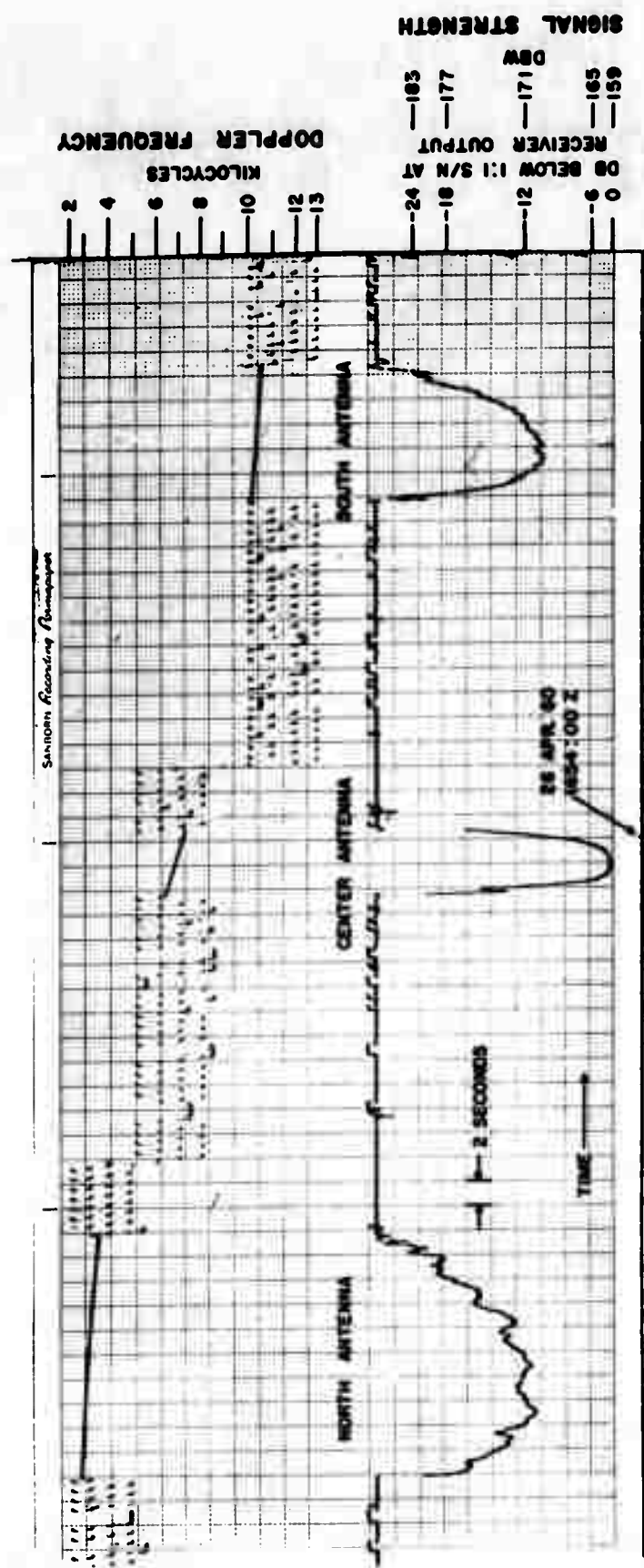


FIG. 33A



ARPA - BRL DOPPLER RECORD OF
60 DELTA REV. 172, FORREST CITY, ARKANSAS
MEASURED 1653:56 Z, PREDICTED 1702 Z
ALTITUDE 77 MILES, 370 MILES EAST FT. SILL
NORTH - CENTER - SOUTH ANTENNAS, NORTH - SOUTH PASS

800

LAUNCH RECORD JUPITER C
JAN. 31, 1958

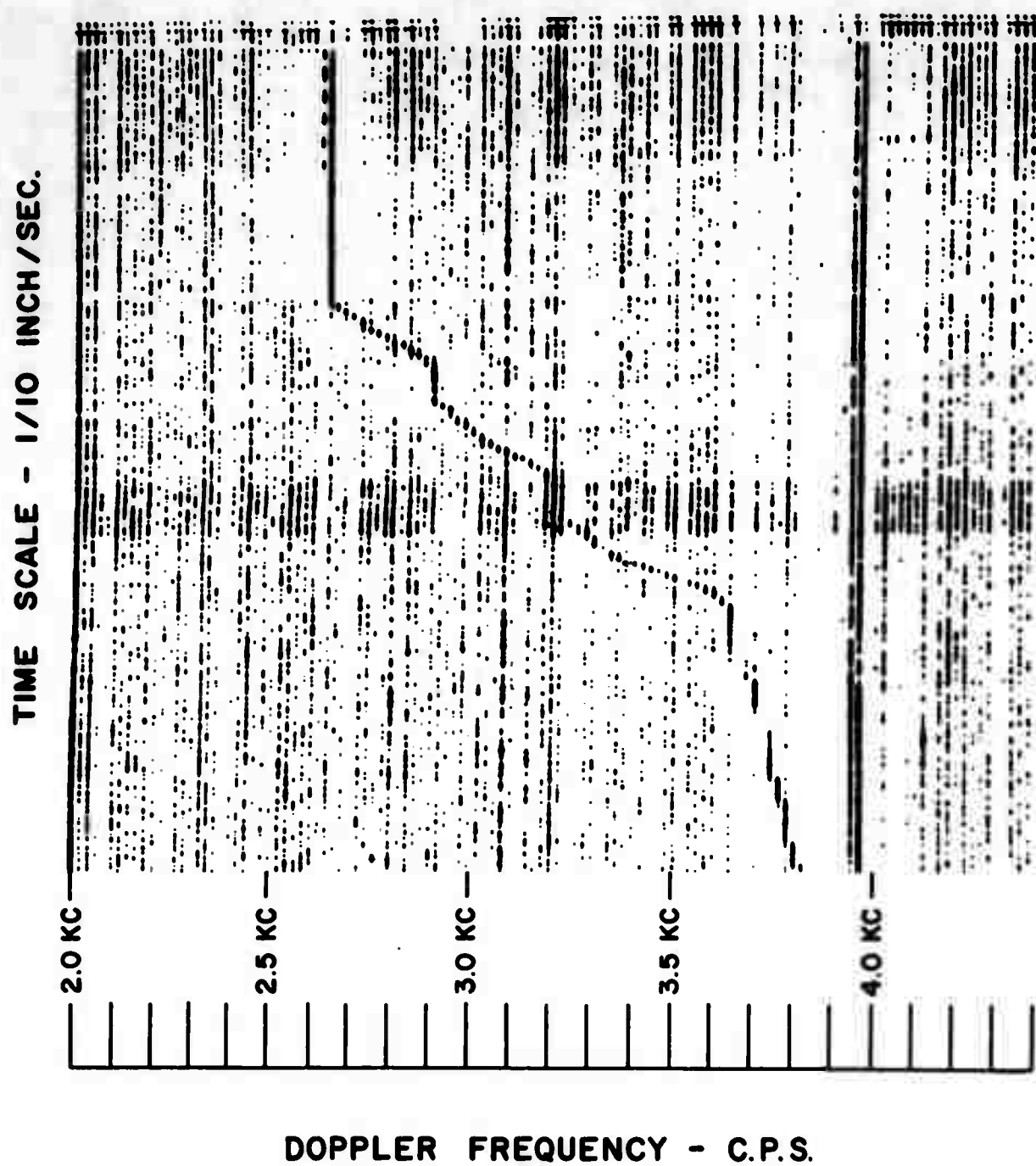


FIG. 34A

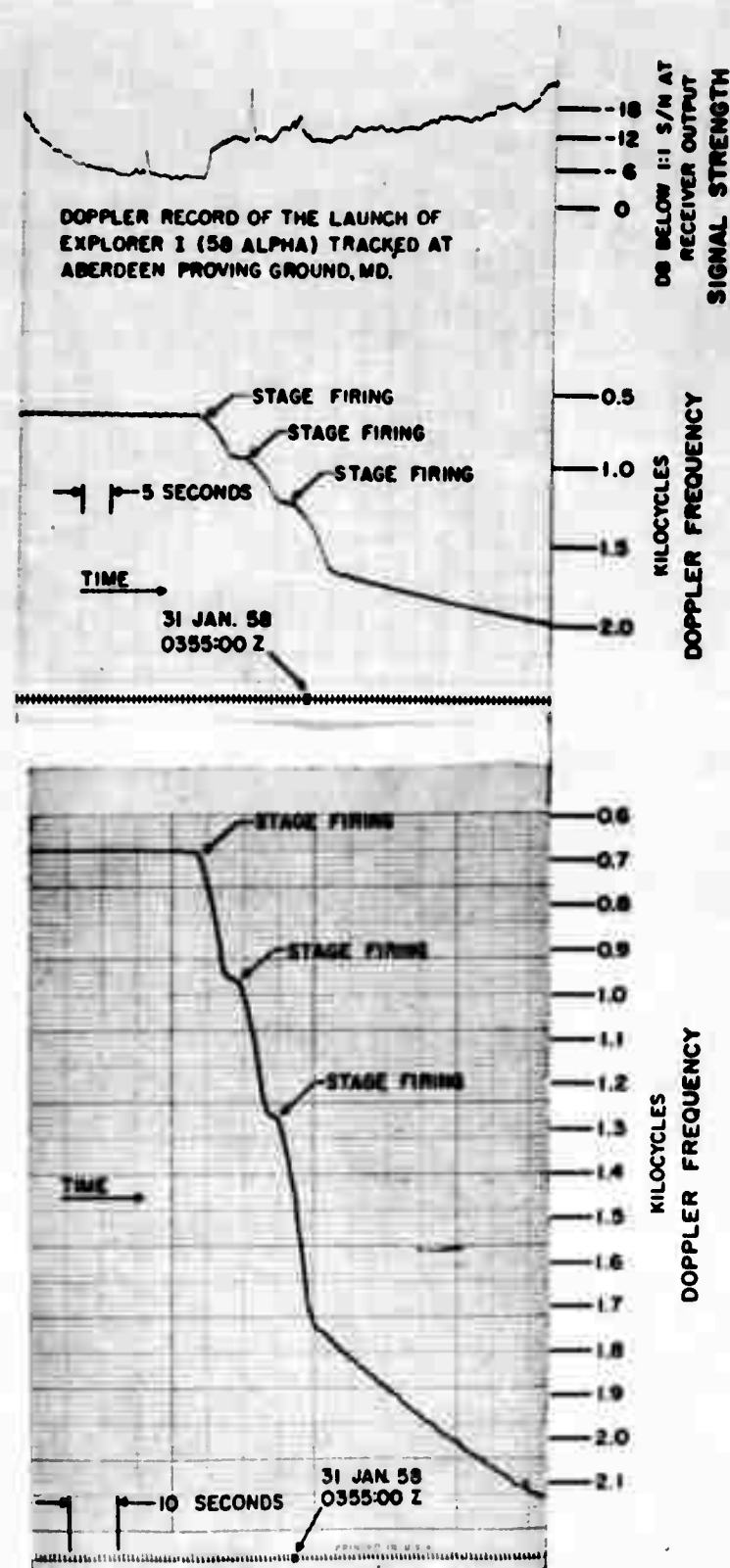


FIG. 348

DOPPLER FREQUENCY RECORD OF THE LAUNCH OF EXPLORER I (58 ALPHA) TRACKED AT ABERDEEN PROVING GROUND, MD.

DISTRIBUTION LIST

<u>No. of Copies</u>	<u>Organization</u>	<u>No. of Copies</u>	<u>Organization</u>
1	Chief of Ordnance ATTN: ORDTB - Bal Sec Department of the Army Washington 25, D. C.	1	Commanding Officer U. S. Communications Agency The Pentagon Washington 25, D. C.
1	Commanding Officer Diamond Ordnance Fuze Laboratories ATTN: Technical Information Office, Branch 041 Washington 25, D. C.	1	Commanding General White Sands Annex - BRL White Sands Missile Range New Mexico
10	Commander Armed Services Technical Information Agency ATTN: TIPCR Arlington Hall Station Arlington 12, Virginia	2	Commanding General Army Ballistic Missile Agency ATTN: Dr. C. A. Lundquist Dr. F. A. Speer Redstone Arsenal, Alabama
10	Commander Air Force Systems Command ATTN: SCTS Andrews Air Force Base Washington 25, D. C.	1	Director Advanced Research Projects Agency Department of Defense Washington 25, D. C.
1	Commander Electronic Systems Division L. G. Hanscom Field Bedford, Massachusetts	1	Director National Aeronautics and Space Administration 1520 H Street, N. W. Washington 25, D. C.
1	Commander Air Proving Ground Center ATTN: PGAPI Eglin Air Force Base, Florida		

<p>AD UNCLASSIFIED Accession No. <u>UNCLASSIFIED</u> UNCLASSIFIED Accession No. <u>UNCLASSIFIED</u></p> <p><u>A COMB FILTER FOR USE IN TRACKING SATELLITES</u></p> <p>Richard L. Vitek</p> <p>ERL Memorandum Report No. 1349 August 1961</p> <p>DA Proj. No. 503-06-011, OMSC No. 5210.11.143</p> <p>UNCLASSIFIED Report</p>	<p><u>Satellites - Detection</u> <u>Radar tracking systems -</u> <u>Recording devices</u> <u>Radar tracking systems -</u> <u>Signal to noise ratio</u></p> <p>This report presents the design and evaluation of a 180 element comb filter. This unit was developed in conjunction with the ARPA Satellite Fence program for the detection and tracking of non-radiating satellites. The primary purpose of this comb filter is to detect and measure the frequency of short duration Doppler signals in the presence of noise. The filter elements have a bandwidth of 10 cps and are spaced 20 cps apart to cover a 3000 cps frequency range. A multiple pen analog recorder is used to record individual filter outputs. The evaluation includes data on simulated as well as actual satellite signals.</p>
<p>AD UNCLASSIFIED Accession No. <u>UNCLASSIFIED</u> UNCLASSIFIED Accession No. <u>UNCLASSIFIED</u></p> <p><u>A COMB FILTER FOR USE IN TRACKING SATELLITES</u></p> <p>Richard L. Vitek</p> <p>ERL Memorandum Report No. 1349 August 1961</p> <p>DA Proj. No. 503-06-011, OMSC No. 5210.11.143</p> <p>UNCLASSIFIED Report</p>	<p><u>Satellites - Detection</u> <u>Radar tracking systems -</u> <u>Recording devices</u> <u>Radar tracking systems -</u> <u>Signal to noise ratio</u></p> <p>This report presents the design and evaluation of a 180 element comb filter. This unit was developed in conjunction with the ARPA Satellite Fence program for the detection and tracking of non-radiating satellites. The primary purpose of this comb filter is to detect and measure the frequency of short duration Doppler signals in the presence of noise. The filter elements have a bandwidth of 10 cps and are spaced 20 cps apart to cover a 3000 cps frequency range. A multiple pen analog recorder is used to record individual filter outputs. The evaluation includes data on simulated as well as actual satellite signals.</p>

<p>AD <u>Wright Research Laboratories, AFGL</u> A COB FILTER FOR USE IN TRACKING SATELLITES Richard L. Vitek HRL Memorandum Report No. 1349 August 1961 DA Proj. No. 503-06-011, QSEC No. 5210.11.143 UNCLASSIFIED Report</p>	<p>UNCLASSIFIED</p> <p>Satellites - Detection Radar tracking systems - Recording devices Radar tracking systems - Signal to noise ratio</p> <p>This report presents the design and evaluation of a 180 element comb filter. This unit was developed in conjunction with the ARPA Satellite Fence program for the detection and tracking of non-radiating satellites. The primary purpose of this comb filter is to detect and measure the frequency of short duration Doppler signals in the presence of noise. The filter elements have a bandwidth of 10 cps and are spaced 20 cps apart to cover a 3800 cps frequency range. A multiple pen analog recorder is used to record individual filter outputs. The evaluation includes data on simulated as well as actual satellite signals.</p>	<p>AD <u>Wright Research Laboratories, AFGL</u> A COB FILTER FOR USE IN TRACKING SATELLITES Richard L. Vitek HRL Memorandum Report No. 1349 August 1961 DA Proj. No. 503-06-011, QSEC No. 5210.11.143 UNCLASSIFIED Report</p>	<p>UNCLASSIFIED</p> <p>Satellites - Detection Radar tracking systems - Recording devices Radar tracking systems - Signal to noise ratio</p> <p>This report presents the design and evaluation of a 180 element comb filter. This unit was developed in conjunction with the ARPA Satellite Fence program for the detection and tracking of non-radiating satellites. The primary purpose of this comb filter is to detect and measure the frequency of short duration Doppler signals in the presence of noise. The filter elements have a bandwidth of 10 cps and are spaced 20 cps apart to cover a 3800 cps frequency range. A multiple pen analog recorder is used to record individual filter outputs. The evaluation includes data on simulated as well as actual satellite signals.</p>
<p>AD <u>Wright Research Laboratories, AFGL</u> A COB FILTER FOR USE IN TRACKING SATELLITES Richard L. Vitek HRL Memorandum Report No. 1349 August 1961 DA Proj. No. 503-06-011, QSEC No. 5210.11.143 UNCLASSIFIED Report</p>	<p>UNCLASSIFIED</p> <p>Satellites - Detection Radar tracking systems - Recording devices Radar tracking systems - Signal to noise ratio</p> <p>This report presents the design and evaluation of a 180 element comb filter. This unit was developed in conjunction with the ARPA Satellite Fence program for the detection and tracking of non-radiating satellites. The primary purpose of this comb filter is to detect and measure the frequency of short duration Doppler signals in the presence of noise. The filter elements have a bandwidth of 10 cps and are spaced 20 cps apart to cover a 3800 cps frequency range. A multiple pen analog recorder is used to record individual filter outputs. The evaluation includes data on simulated as well as actual satellite signals.</p>	<p>AD <u>Wright Research Laboratories, AFGL</u> A COB FILTER FOR USE IN TRACKING SATELLITES Richard L. Vitek HRL Memorandum Report No. 1349 August 1961 DA Proj. No. 503-06-011, QSEC No. 5210.11.143 UNCLASSIFIED Report</p>	<p>UNCLASSIFIED</p> <p>Satellites - Detection Radar tracking systems - Recording devices Radar tracking systems - Signal to noise ratio</p> <p>This report presents the design and evaluation of a 180 element comb filter. This unit was developed in conjunction with the ARPA Satellite Fence program for the detection and tracking of non-radiating satellites. The primary purpose of this comb filter is to detect and measure the frequency of short duration Doppler signals in the presence of noise. The filter elements have a bandwidth of 10 cps and are spaced 20 cps apart to cover a 3800 cps frequency range. A multiple pen analog recorder is used to record individual filter outputs. The evaluation includes data on simulated as well as actual satellite signals.</p>

UNCLASSIFIED

UNCLASSIFIED